

A robust optimization approach to flow decomposition

Moritz Stinzenhöfer^{1,2}, Philine Schiewe¹, and Fabricio Oliveira¹

¹Systems Analysis Laboratory Department of Mathematics and Systems Analysis,
Aalto University, Otakaari 1, 02150 Espoo, Finland

²Department of Mathematics, RPTU Kaiserslautern-Landau, Paul-Ehrlich-Str. 14,
67663 Kaiserslautern, Germany

October 29, 2024

Abstract In this paper, we consider a variant of the so-called minimum flow decomposition (MFD) problem in which uncertainty regarding edge capacities is taken into account from a robustness perspective. In the classical flow decomposition problem, a network flow is decomposed into a set of weighted paths from a fixed source node to a fixed sink node that precisely represents the flow distribution across all edges. While MFDs are often used in bioinformatics applications, they are also applicable in other fields, such as flows of goods or passengers in distribution networks, where the decomposition represents the vehicles and corresponding capacities needed to cover these flows. We generalize this problem to the weighted inexact case with lower and upper bounds on the flow values, provide a detailed analysis, and explore different variants that are solvable in polynomial time. Moreover, we introduce the concept of robust flow decomposition by incorporating uncertain flows and applying different robustness concepts to handle the uncertainty. Finally, we present two different adjustable problem formulations and perform computational experiments illustrating the benefit of adjustability in the uncertain case in a subsequent computational study.

Keywords flow decomposition, uncertainty, robust optimization

1 Introduction

Network flows are a fundamental concept in mathematics, particularly in the field of graph theory and optimization. A network is typically represented as a directed graph, with nodes representing junctions or points of interest and edges representing the pathways or connections between these nodes. The primary goal in network flow problems is typically to determine the optimal way to send a certain amount of flow from a source node to a sink node or to find the minimum cost flow. In the latter, each edge has a cost associated with transporting flow through it, and the objective is to minimize the total cost while satisfying flow requirements. These network flow problems have wide-ranging applications in fields such as transportation [BK09], telecommunications [LSBG13], logistics [SB22], and bioinformatics [WRM19], making them an essential area of study in both theoretical and applied mathematics.

Another important network flow problem is the minimum flow decomposition (MFD), which involves decomposing the flow into a set of weighted paths that represent how the flow is distributed through the network. This is often applied in bioinformatics applications such as multiassembly problems [DWMT22], which involve reconstructing genomic sequences from short substrings. In RNA transcript assembly, for example, sequenced substrings are used to construct weighted graphs where nodes represent exons and edges represent connections between them. These graphs aim to find a set of weighted paths that best explain the graph's weights, a task at which the MFD excels under ideal conditions. However, practical data often contain uncertainties and measurement errors, making it challenging to form accurate flow networks, which is why the related research focuses on robustness against measurement errors [DT23]. Robustness in the sense that the solution is robust against all possible realizations within an uncertainty set is more relevant in transportation problems, such as public transport planning, where MFDs are also useful. Public transport planning involves several

stages, including line planning, timetabling, and vehicle scheduling. The latter stage, in particular, can benefit from the MFD by decomposing trip graphs into a minimal number of paths, optimizing vehicle utilization, and reducing operational costs. Despite the extensive literature on robustness considerations in public transport planning, most research focuses on timetabling and delay management, considering uncertainties like travel times or disruptions. Demand uncertainties are often addressed in earlier planning stages or in other applications like vehicle routing problems. In contrast, in this paper, we explore the minimum flow decomposition problem (MFDP) within the framework of robust optimization and propose the definition of a *robust flow decomposition*. To the best of our knowledge, this is the first work in this direction.

The main contributions of the paper can be summarized as follows:

- we examine existing variants of MFDP with regard to different robustness concepts,
- we generalize the MFDP to the weighted inexact case with lower and upper bounds on the flow values, investigate the complexity of the resulting problem, and explore different variants that are solvable in polynomial time,
- we introduce the concept of robust flow decomposition by incorporating uncertain flows and discuss special cases with different robustness concepts,
- and we present two different adjustable problem formulations for which we develop a proof of concept highlighting the benefit of adjustability in the uncertain case in a subsequent computational study.

The remainder of this paper is structured as follows: The connections to the related literature are discussed in Section 2 while we give some underlying definitions and revisit the MFDP and its variations in the context of robust optimization in Section 3. In Section 4, we introduce the generalized deterministic problem and discuss the complexities of relevant variants as well as their strictly robust counterparts. Further, we propose two adjustable problem formulations in Section 5 followed by a corresponding computational study in Section 6. Section 7 concludes the paper.

2 Literature review

Covering nodes, edges, or paths in a graph is a common problem that appears in many well-studied concepts in areas of graph theory and network analysis. One example is to find a *minimum path cover (MPC)*, i.e., a set of directed paths with minimum cardinality that covers all vertices (or edges), in a digraph [Die05]. Since the MPC consists of one path if and only if there is a Hamiltonian path in the corresponding graph, the MPC problem is NP-hard.

However, unlike the MFDP and its robust variants we investigate, the edges only need to be covered by a minimum number of paths, and there are no flow values that have to match weights associated with the paths. Therefore, the MPC can be solved in polynomial time if the graph is acyclic, e.g., by transforming it into a matching problem [NH79].

The *flow decomposition problem (FDP)* [AMO88], on the other hand, describes the problem of decomposing a network flow into a set of weighted paths from a fixed source node to a fixed sink node that precisely represents the flow distribution across all edges. One way to compute such a flow decomposition in a *directed acyclic graph (DAG)* is to iteratively remove weighted paths that utilize at least one edge. The authors of [AMO88] show that this results in a flow decomposition with at most $|E|$ paths (where $|E|$ is the number of edges in the graph) and can be computed in polynomial time. Nonetheless, when aiming to minimize the number of paths in the decomposition, referred to as *minimum flow decomposition (MFD)*, the problem becomes NP-hard [VCCM08] and is even hard to approximate [HHK⁺12]. As a result, efficient heuristics have been developed, such as the greedy methods in [VCCM08] or an improved version in [SK17]. In the former, the proposed algorithms iteratively choose the shortest path or the path with the largest flow value in the remaining flow until the entire flow is decomposed, while in the latter, the flow graph is first modified before applying the greedy method.

Recently, the authors of [DWMT22] presented an exact solution approach for the MFDP on DAGs, which is based on an integer linear programming (ILP) approach using only a quadratic number of variables instead of enumerating all possible paths in the network (which would lead to an exponential

number of variables). They show that their proposed method consistently solves instances on both simulated and real datasets significantly faster than previous approaches. These data sets originate from applications in bioinformatics, such as *multiassembly problems*, where MFD plays a key role [XRL04].

The multiassembly problem involves reconstructing various genomic sequences from short substrings (called sequenced *reads*) [XRL04], such as RNA transcript assembly [LFJ11, SK17], i.e., recovering the set of full-length transcripts. Initially, reads are used to construct a weighted graph, like a splicing graph in RNA transcript assembly, where nodes represent exons, and edges denote connections between them. These edges, nodes, or both are weighted, typically indicating average read coverage. The multiassembly problem is then about finding a set of weighted paths that best explain the graph’s weights [TGP⁺15, SK17], and it has been shown that the MFD has a very high accuracy on perfect data [DT23]. However, since the assumption of perfect data is often not given in practice due to different sources of uncertainty and measurement errors, splice graphs derived from experimental data are unlikely to form a flow network [WRM19]. To address this problem, the authors of [WRM19] assign intervals of possible weights to the edges instead of exact weights, which forms a so-called *inexact flow network*. The resulting problem of identifying a minimal set of paths that explain these intervals is called the *minimum inexact flow decomposition problem (MIFDP)* and is also considered in [DWMT22] by a slight modification of the exact MFD solver. Other approaches aim to identify a minimum set of weighted paths that minimizes the sum of squared differences between the weight of each edge and the sum of weights of paths passing through it or to assign slack variables to each path to move error handling away from the individual edges [DT23]. All these approaches have in common that they try to be robust against possible measurement errors. This means that although all data is known, it is likely to be error-prone, which is why, in most cases, no classical flow decomposition can be achieved. However, to ensure that the paths in the decomposition form feasible flows, the requirement that the measured weight of each edge and the sum of weights of paths passing through it must match is relaxed. In contrast to the typical assumptions in robust optimization, a scenario or the real data is not revealed here. While this is suitable from a bioinformatics point of view, robustness in the classical sense of finding a feasible solution that is robust for every possible realization in an uncertainty set is more applicable to transportation problems or public transport planning, where the MFD also plays a key role.

In public transport planning, the operational costs are mainly determined by the *vehicle schedule* [SS22], which is part of the traditional sequential planning approach [HKL05, GH08]. Typically, this begins on a strategic level with a demand analysis to build passenger demand matrices, which are then used to define the overall structure of the transit network, including necessary infrastructure such as stations or depots. In the next step, called *line planning*, the types of services (e.g., bus, rail, tram) and their routes, stops, and frequencies are determined to meet the demand and policy goals [Sch12]. This is followed by the operational planning stage, where the *timetabling* step focuses on creating detailed schedules for each line, resulting in so-called *trips* with departure and arrival times for each station as well as start and end stations [LLER11]. Then, vehicle scheduling allocates vehicles to trips, ensuring that all scheduled trips are covered while optimizing vehicle utilization, often characterized by minimal fleet size or operational costs [BK09]. The former can be addressed by decomposing the trip graph into a minimal number of paths [BK09] and also, in recent applications such as electric buses with limited driving ranges, decomposition methods are used for vehicle scheduling [OKW22]. Although there is a lot of literature dedicated to robustness in public transport, most of it concentrates on timetabling and delay management by considering uncertain travel times or disruptions [CT12, PNP16, LLB18]. Demand uncertainties are often considered in earlier stages, e.g., stop panning [CQY20], or in other applications such as *vehicle routing problems* [LLP12].

To handle uncertainties in mathematical problems generally, the concept of *robust optimization* was introduced [Soy73, BTN98], which usually refers to finding an optimal solution that is feasible for all possible realizations (often represented as scenarios) induced by an uncertainty set. For an extensive overview of theoretical properties and applications, we refer the reader to [BS07, BBC11, GMT14]. Instead of finding the best robust solution for the worst-case scenario, in *regret robustness* [KY13], the objective is to minimize the difference (*regret*) between the robust solution value and the best objective value we could have achieved if the realization had been known beforehand. Since these approaches still require the solution to be feasible for all possible scenarios, the concept of *light robustness* [Sch14] weakens the feasibility constraint by only searching for solutions that are feasible and ”good enough”

in the *nominal case* (e.g., the most likely case). An alternative idea to overcome over-conservatism is to bound the uncertainty set by parameterizing the allowed cumulative deviation from the nominal case, resulting in a *budgeted uncertainty set* [BS04]. A similar approach is followed for the *optimization problems under controllable uncertainty* [LMM⁺23], where the uncertainty is allowed to be reduced at a given cost. As it is possible in many applications to adjust a part of the decisions after observing the scenario, the concept *adjustable robustness* [BTGGN04] takes this into account. The idea is to divide the variables into those that must be decided before the scenario is unveiled and those that can be decided after the realization. For an overview, we refer to [YGDH19].

As previous concepts mainly concentrate on applications in bioinformatics, the focus to date has primarily been on dealing with data inaccuracies. To the best of our knowledge, this is the first work that considers MFDs in the context of classical robustness concepts. This opens up many other application possibilities that are typically represented using flow networks and in which uncertainty plays a role. In public transport, for example, it is now also possible to take demand uncertainties into account in later planning steps such as vehicle scheduling. In general, this allows robust and, depending on the application, resource-efficient solutions to be achieved despite uncertain data.

3 Technical background

Before considering our problem formulations, we introduce the underlying deterministic model and its alternative robust variants.

3.1 Minimum flow decomposition

In this section, we follow the definitions in [DWMT22]. Let $G(V, E)$ be a digraph with no directed cycles (DAG), where $s \in V$ represents the *source* node with no incoming edges and $t \in V$ the *sink* (*target*) node with no outgoing edges. Let f_{uv} be the corresponding non-negative integer flow value of edge (u, v) for all $(u, v) \in E$, i.e., $f : E \rightarrow \mathbb{N}_{\geq 0}$. Definition 1 provides a formal description of a *flow network*. An example of a flow network can be found in Figure 1a.

Definition 1 (Flow network). *The tuple $G(V, E, f)$ is called a flow network if for every $v \in V \setminus \{s, t\}$ the conservation of flow*

$$\sum_{u:(u,v) \in E} f_{uv} = \sum_{w:(v,w) \in E} f_{vw} \quad (1)$$

is satisfied.

Given such a flow network, it can be decomposed into a set of $s - t$ -paths, where each path has an associated positive weight (Figure 1b). Definition 2 describes how $s - t$ -paths form a k -flow decomposition.

Definition 2 (k -flow decomposition). *For a given flow network $G(V, E, f)$, a set of $s - t$ -paths $\mathcal{P} = (P_1, \dots, P_k)$ with corresponding positive weights $w = (w_1, \dots, w_k)$ is called k -flow decomposition if*

$$\sum_{i:(u,v) \in P_i} w_i = f_{uv} \quad (2)$$

holds for all $(u, v) \in E$.

The *value* $|f|$ of a flow f is the *net flow* $\sum_{u:(u,t) \in E} f_{ut}$ into the sink node t [GTT89]. As we assume integer flow values, there is the trivial $|f|$ -flow decomposition with $|f|$ paths of weight one [AMO88]. Consequently, we can bound k by the flow value $|f|$.

Problem 3 (Minimum flow decomposition problem). *For a given flow network $G(V, E, f)$, the minimum flow decomposition problem (MFDP) is to find a k -flow decomposition $\mathcal{P} = (P_1, \dots, P_k)$ such that k is minimized.*

For a given upper bound \bar{K} of k (e.g., $|f|$), we can formulate the corresponding MIP formulation in (3), which is essentially the formulation in [DWMT22].

$$\min_{x, y, w} \sum_{i=1}^{\overline{K}} y_i \quad (3a)$$

$$\text{s.t.} \quad \sum_{v:(s,v) \in E} x_{svi} = y_i, \quad \forall i \in \{1, \dots, \overline{K}\}, \quad (3b)$$

$$\sum_{u:(u,t) \in E} x_{uti} = y_i, \quad \forall i \in \{1, \dots, \overline{K}\}, \quad (3c)$$

$$\sum_{(u,v) \in E} x_{uvi} - \sum_{(v,w) \in E} x_{vwi} = 0, \quad \forall i \in \{1, \dots, \overline{K}\}, v \in V \setminus \{s, t\}, \quad (3d)$$

$$\sum_{i \in \{1, \dots, \overline{K}\}} w_i x_{uvi} = f_{uv}, \quad \forall (u, v) \in E, \quad (3e)$$

$$w_i \in \mathbb{Z}^+, \quad \forall i \in \{1, \dots, \overline{K}\}, \quad (3f)$$

$$x_{uvi} \in \{0, 1\}, \quad \forall (u, v) \in E, i \in \{1, \dots, \overline{K}\}, \quad (3g)$$

$$y_i \in \{0, 1\}, \quad \forall i \in \{1, \dots, \overline{K}\}. \quad (3h)$$

Here, the binary variable y_i indicates whether the path i with the corresponding weight $w_i \in \mathbb{Z}^+$ is part of the flow decomposition ($y_i = 1$) or not ($y_i = 0$) and $x_{uvi} \in \{0, 1\}$ is equal to one if edge $(u, v) \in E$ is used by path $i \in \{1, \dots, \overline{K}\}$. Note that (3) is formally an MIP only if we linearize constraints (3e). For further details, we refer the reader to [DWM22]. Example 4 illustrates the aforementioned definitions.

Example 4 ([DT23]). Assume we are given the graph in Figure 1a with flow values on the corresponding edges. Then this flow network can be decomposed into the five colored paths P_1, P_2, P_3, P_4, P_5 shown in Figure 1b with the associated weights $w_1 = 1, w_2 = 2, w_3 = 2, w_4 = 2, w_5 = 3$. Moreover, this is an optimal solution to MFDP with a solution value of $k = 5$.

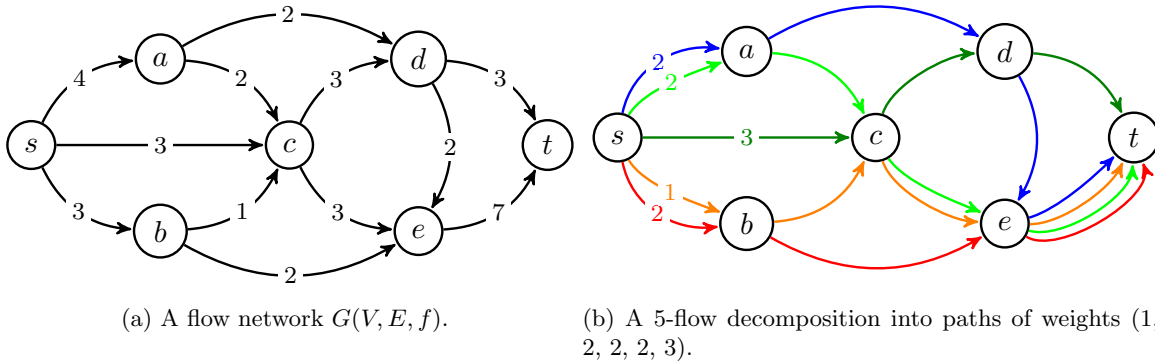


Figure 1: Example of a flow network and a flow decomposition into 5 $s - t$ -paths [DT23].

The MFDP can be generalized by relaxing constraints (3e), allowing the summed path weights of each edge (u, v) to lie in a range $[f_{uv}^l, f_{uv}^u]$ instead of matching a flow value f_{uv} . Consequently, the underlying graph is now an *inexact flow network* [WRM19], meaning that we have a lower bound f_{uv}^l and an upper bound flow value f_{uv}^u corresponding to each edge $(u, v) \in E$. The resulting problem is summarized in the following.

Problem 5 (Minimum inexact flow decomposition problem [WRM19]). For a given inexact flow network $G(V, E, f^l, f^u)$, the minimum inexact flow decomposition problem (MIFDP) is to find a set of $s - t$ -paths $\mathcal{P} = (P_1, \dots, P_k)$ with minimum cardinality and associated positive weights $w = (w_1, \dots, w_k)$ such that

$$f_{uv}^l \leq \sum_{i:(u,v) \in P_i} w_i \leq f_{uv}^u \quad (4)$$

holds for all $(u, v) \in E$. We obtain its corresponding MIP formulation by replacing constraints (3e) in (3) with (5)

$$\begin{aligned} \sum_{i \in \{1, \dots, \bar{K}\}} w_i x_{uvi} &\geq f_{uv}^l \quad \forall (u, v) \in E, \\ \sum_{i \in \{1, \dots, \bar{K}\}} w_i x_{uvi} &\leq f_{uv}^u \quad \forall (u, v) \in E. \end{aligned} \quad (5)$$

Note that both MFDP and its generalization, MIFDP, are NP-hard [DT23].

3.2 Robustness considerations

As we want to provide formulations that can take into account the uncertainty associated with MFD flow values, we make use of three different notions of robustness, which can be found in the literature. The first is broadly referred to in the literature as *robust optimization* [BTN98, BTEGN09], which we hereinafter call *strict robustness* as in [WCL18].

For a given optimization under uncertainty problem of the form

$$\begin{aligned} \min_x \quad & f(x) \\ \text{s.t.} \quad & F(x, \xi) \leq 0, \\ & x \in \mathbb{R}^n, \end{aligned} \quad (6)$$

with $f(\cdot) : \mathbb{R}^n \rightarrow \mathbb{R}$ and $F(\cdot, \xi) : \mathbb{R}^n \rightarrow \mathbb{R}^m$ for some uncertain parameter ξ whose possible realizations are assumed to lie within an uncertainty set $\mathcal{U} \subset \mathbb{R}^N$, the *strictly robust counterpart* is defined by

$$\begin{aligned} \min_x \quad & f(x) \\ \text{s.t.} \quad & F(x, \xi) \leq 0 \quad \forall \xi \in \mathcal{U}, \\ & x \in \mathbb{R}^n. \end{aligned} \quad (7)$$

An optimal solution to (7) is called a *strictly robust solution*, i.e., we search for the best solution that is feasible for all scenarios $\xi \in \mathcal{U}$.

Since we are dealing with interval-wise uncertainty in the following, we can define the scenarios according to the deviation from a nominal scenario $\hat{\xi}$ (e.g., the expected value or the most likely scenario). This means that \mathcal{U} is of the form

$$\mathcal{U} = \left\{ \xi \in \mathbb{R}_{\geq 0}^N : \xi_i \in [\hat{\xi}_i - \underline{\delta}_i, \hat{\xi}_i + \bar{\delta}_i], \forall i \in \{1, \dots, N\} \right\}, \quad (8)$$

for given $\underline{\delta}, \bar{\delta} \in \mathbb{R}_{\geq 0}^N$, where ξ_i corresponds to the i -th entry of scenario ξ .

Strict robustness is often too conservative, especially regarding the requirement that the solution be feasible for all scenarios within the uncertainty set. As a result, the literature is rich in alternative forms of robustness, which have also been investigated [BS07, GMT14].

To prevent the uncertainty set from leading to over-conservative solutions, the cumulative deviation from the nominal scenario can be bounded by the uncertainty budget $\Gamma \in \mathbb{R}_{\geq 0}$. To be more precise, $\mathcal{U}(\Gamma)$ is of the form

$$\mathcal{U}(\Gamma) = \left\{ \xi \in \mathbb{R}_{\geq 0}^N : \xi_i \in [\hat{\xi}_i - \underline{\delta}_i, \hat{\xi}_i + \bar{\delta}_i], \forall i \in \{1, \dots, N\}; \sum_{j=1}^N |\xi_j - \hat{\xi}_j| \leq \Gamma \right\}. \quad (9)$$

This is known as *cardinality-constraint uncertainty set* or *budgeted uncertainty set* [BS04] and we will refer to it as Γ -*uncertainty set* (referring to the uncertainty budget Γ).

In some cases, it is reasonable to assume that part of the decisions, the so-called *wait-and-see decisions*, can be made after the scenario ξ is revealed, while the *here-and-now decisions* have to be decided before the scenario ξ is observed. More formally, we can distinguish between *non-adjustable variables* $u \in \mathbb{R}^p$ (here-and-now decisions, as in the strict robust case) and *adjustable variables* $v \in \mathbb{R}^q$,

whose values may depend on the realization ξ . This concept is called *adjustable robustness* [BTGGN04] and for $x = (u, v) \in \mathbb{R}^n$ the *adjustable robust counterpart* of (7) is defined as

$$\begin{aligned} \min_u \quad & \inf_{v \in \mathbb{R}^q} f(u, v) \\ \text{s.t.} \quad & F(u, v, \xi) \leq 0 \quad \forall \xi \in \mathcal{U}, \\ & u \in \{u \in \mathbb{R}^p : \forall \xi \in \mathcal{U} \exists v \in \mathbb{R}^q : F(u, v, \xi) \leq 0\}, \end{aligned} \quad (10)$$

with $p + q = n$. This means that we fix the non-adjustable variables u , observe ξ , and then make a decision on the adjustable variables v depending on the scenario ξ and u . An optimal solution to (10) is called an *adjustable robust solution*. Note that for $p = n$, i.e., $x = u \in \mathbb{R}^n$, the adjustable robust counterpart (10) reduces to the strictly robust counterpart (7).

3.3 Applying the notion of strict robustness to the MFDP and MIFDP

When considering uncertainty and (inexact) flow networks in general, it is natural that the flow values are the source of uncertainty. If we apply the notion of strict robustness to the MFDP with uncertain flows, the strictly robust counterpart (7) becomes infeasible if there are at least two different scenarios $f' \neq f'' \in \mathcal{U}$ since there is at least one (u, v) with $f'_{uv} \neq f''_{uv}$ and constraints (3e) cannot be fulfilled.

In general, this is not the case for the MIFDP since the summed path weights of each edge (u, v) must lie within a range $[f'_{uv}, f''_{uv}]$ instead of matching exactly a flow value f_{uv} . Consequently, it is possible that different scenarios $f' \neq f'' \in \mathcal{U}$ form a feasible combination of constraints in (5) that an inexact flow can fulfill.

Since we are dealing with non-negative integer flows, non-integer bounds on the flow values can also be reduced to integers by rounding up or down. Consequently, it is sufficient to consider a discrete uncertainty set consisting of values in $\mathbb{N}_{\geq 0}$ since any other uncertainty set for this problem can be reduced to its discrete version. Therefore, we set

$$\mathcal{U} = \left\{ (f^{l,\xi}, f^{u,\xi}) \in \left(\mathbb{N}_{\geq 0}^{|E|} \right)^2 : \xi = 1, \dots, N \right\}, \quad (11)$$

i.e., we have $|\mathcal{U}|$ scenarios, each scenario ξ consisting of a lower $f_e^{l,\xi}$ and an upper bound $f_e^{u,\xi}$ for all edges $e \in E$ (w.l.o.g. $f_e^{l,\xi} \leq f_e^{u,\xi}$).

With this definition, we do not necessarily consider interval-wise uncertainty but also any other finite uncertainty sets. Thus, it is possible that no strictly robust solution exists if there is at least one edge e for which the intersection of the intervals $[f_e^{l,\xi}, f_e^{u,\xi}]$ of all scenarios ξ is empty, i.e., there is no flow value f with $f \in [f_e^{l,\xi}, f_e^{u,\xi}]$ for all $\xi \in \mathcal{U}$. However, since we are interested in strictly robust solutions in this section, we assume that such solutions exist, i.e., in particular, that there is a flow value f such that $f \in [f_e^{l,\xi}, f_e^{u,\xi}]$ holds for all $\xi \in \mathcal{U}$ and $e \in E$. With this assumption, the uncertainty set can be reduced to an interval-wise uncertainty set for the strictly robust case.

Strict robustness considering the uncertainty set \mathcal{U} Therefore, we can assume that

$$\mathcal{U} = \left\{ (f^l, f^u) \in \left(\mathbb{N}_{\geq 0}^{|E|} \right)^2 : f_{uv}^l \in [f_{uv}^l, \bar{f}_{uv}^l], f_{uv}^u \in [f_{uv}^u, \bar{f}_{uv}^u], \forall (u, v) \in E \right\}, \quad (12)$$

being an interval-wise uncertainty set with given $f^l, \bar{f}^l, f^u, \bar{f}^u \in \mathbb{N}_{\geq 0}^{|E|}$. Note that since the flow values are integers, (11) contains (12) and can be constructed by enumerating all elements in an interval-wise uncertainty set.

Lemma 6. *For the strictly robust counterpart of MIFDP, the uncertainty set \mathcal{U} can be reduced to $\mathcal{U} = \{(f^l, f^u)\}$ with $f_{uv}^l = \bar{f}_{uv}^l$ and $f_{uv}^u = \bar{f}_{uv}^u$ for all $(u, v) \in E$.*

Proof. Every feasible solution to MIFDP with $f_{uv}^l = \bar{f}_{uv}^l$ and $f_{uv}^u = \bar{f}_{uv}^u$ for all $(u, v) \in E$ (w.l.o.g. there is at least one) is feasible for all other scenarios $(f^l, f^u) \in \mathcal{U}$. This means $(f^l, f^u) = (\bar{f}^l, \bar{f}^u)$ can be seen as a worst-case scenario, and the problem can be reduced to this particular case. Consequently, every optimal solution to MIFDP with $f_{uv}^l = \bar{f}_{uv}^l$ and $f_{uv}^u = \bar{f}_{uv}^u$ for all $(u, v) \in E$ is a strictly robust solution. \square

Strict robustness regarding Γ -uncertainty set $\mathcal{U}(\Gamma)$ If we restrict \mathcal{U} in (12) to a Γ -uncertainty set $\mathcal{U}(\Gamma)$, i.e., $\mathcal{U}(\Gamma)$ must fulfill

$$\sum_{(u,v) \in E} |f_{uv}^l - \hat{f}_{uv}^l| + |f_{uv}^u - \hat{f}_{uv}^u| \leq \Gamma \quad (13)$$

concerning a nominal scenario (\hat{f}^l, \hat{f}^u) with $\hat{f}_{uv}^l \in [f_{uv}^l, \bar{f}_{uv}^l]$ and $\hat{f}_{uv}^u \in [f_{uv}^u, \bar{f}_{uv}^u]$ for $(u, v) \in E$, the resulting worst-case scenario is only slightly different.

Lemma 7. *For the strictly robust counterpart of MIFDP, the Γ -uncertainty set $\mathcal{U}(\Gamma)$ can be reduced to $\mathcal{U}(\Gamma) = \{(f^l, f^u)\}$ with $f_{uv}^l = \min\{\hat{f}_{uv}^l + \Gamma, \bar{f}_{uv}^l\}$ and $f_{uv}^u = \max\{\hat{f}_{uv}^u - \Gamma, \underline{f}_{uv}^u\}$ for all $(u, v) \in E$.*

Proof. Since we are deciding not only on the number of paths but also on the paths themselves, once both decisions have been made, they have to be feasible for all scenarios. Consequently, for every $\Gamma \geq 0$, we can find a set of realizations so that for each $(u, v) \in E$, there is at least one realization with $f_{uv}^l = \min\{\hat{f}_{uv}^l + \Gamma, \bar{f}_{uv}^l\}$ and at least one with $f_{uv}^u = \max\{\hat{f}_{uv}^u - \Gamma, \underline{f}_{uv}^u\}$. Since the robust solution has to be feasible for any realization, a scenario that covers all worst-case scenarios is $(f_{uv}^l, f_{uv}^u) = (\min\{\hat{f}_{uv}^l + \Gamma, \bar{f}_{uv}^l\}, \max\{\hat{f}_{uv}^u - \Gamma, \underline{f}_{uv}^u\})$ for all $(u, v) \in E$. Note that this particular scenario is not necessarily part of $\mathcal{U}(\Gamma)$. \square

As we have seen, after applying the notion of strict robustness to both MFDP and MIFDP, the strictly robust counterparts are either infeasible or can be solved by reducing the uncertainty set to one scenario. Therefore, we propose a generalization of both in the following sections, which is suitable for a more detailed analysis.

4 Minimum weighted inexact flow decomposition problem

In this section, we introduce a generalized version of the MIFDP by minimizing the weighted sum of the associated weights $a_w \sum_{i=1}^{|\mathcal{P}|} w_i$ in addition to the number of paths $a_y |\mathcal{P}|$. Since both now occur with corresponding weights $a_y, a_w \in \mathbb{R}_{\geq 0}$ in the objective function, it motivates the analysis of the subproblems resulting from different weight combinations. While $a_y > 0, a_w = 0$ corresponds to the MIFDP, we show how $a_y = 0, a_w > 0$ can be solved in polynomial time. Moreover, polynomial time can also be achieved for $a_y > 0, a_w = 0$ if the upper bounds on the flow values are neglected. Utilizing these results, we show how the corresponding strictly robust counterparts of the described variants can be solved in polynomial time.

4.1 General formulation

Using the MIFDP as a starting point, the weight variables w no longer necessarily match the flow values since the summed path weights of each edge (u, v) lie in a range $[f_{uv}^l, f_{uv}^u]$ instead. Depending on the magnitude of the upper bounds in f^u , the entries of w can take on large values, even if smaller ones would be sufficient to cover the corresponding lower bounds. Therefore, it is reasonable to extend the objective function by the sum of all weights, as in many related applications, the weights are desired to be as small as possible, e.g., if they correspond to a vehicle's capacity. The resulting problem is formalized in the following.

Problem 8 (Minimum weighted inexact flow decomposition problem). *For a given inexact flow network $G(V, E, f^l, f^u)$, the minimum weighted inexact flow decomposition problem (MWIFDP) is to find a set of $s - t$ -paths $\mathcal{P} = (P_1, \dots, P_k)$ with associated positive weights $w = (w_1, \dots, w_k)$ such that*

$$f_{uv}^l \leq \sum_{i:(u,v) \in P_i} w_i \leq f_{uv}^u$$

holds for all $(u, v) \in E$ and the weighted sum

$$a_y |\mathcal{P}| + a_w \sum_{i=1}^{|\mathcal{P}|} w_i, \quad (14)$$

with weights $a_y, a_w \in \mathbb{R}_{\geq 0}$ is minimized.

For a given upper bound \bar{K} of k , the corresponding MIP formulation is given by

$$\min_{x, y, w} \sum_{i=1}^{\bar{K}} (a_y y_i + a_w w_i) \quad (15a)$$

$$\text{s.t.} \quad \sum_{v:(s,v) \in E} x_{svi} = y_i, \quad \forall i \in \{1, \dots, \bar{K}\}, \quad (15b)$$

$$\sum_{u:(u,t) \in E} x_{uti} = y_i, \quad \forall i \in \{1, \dots, \bar{K}\}, \quad (15c)$$

$$\sum_{(u,v) \in E} x_{uvi} - \sum_{(v,w) \in E} x_{vwi} = 0, \quad \forall i \in \{1, \dots, \bar{K}\}, v \in V \setminus \{s, t\}, \quad (15d)$$

$$\sum_{i \in \{1, \dots, \bar{K}\}} w_i x_{uvi} \geq f_{uv}^l, \quad \forall (u, v) \in E, \quad (15e)$$

$$\sum_{i \in \{1, \dots, \bar{K}\}} w_i x_{uvi} \leq f_{uv}^u, \quad \forall (u, v) \in E, \quad (15f)$$

$$w_i \in \mathbb{Z}^+, \quad \forall i \in \{1, \dots, \bar{K}\}, \quad (15g)$$

$$x_{uvi} \in \{0, 1\}, \quad \forall (u, v) \in E, i \in \{1, \dots, \bar{K}\}, \quad (15h)$$

$$y_i \in \{0, 1\}, \quad \forall i \in \{1, \dots, \bar{K}\}. \quad (15i)$$

Note that it is easy to add symmetry-breaking constraints to (15).

Obviously, MWIFDP reduces to MFDP for $a_y > 0$ and $a_w = 0$ and is therefore NP-hard. But this is also the case for $a_y, a_w > 0$, as shown in the following lemma.

Lemma 9. *For $a_y, a_w > 0$, MWIFDP is NP-hard since it includes the MFDP.*

Proof. Given an instance $G(V, E, f)$ of MFDP, we can construct an instance $G(V, E, f^l, f^u)$ of MWIFDP using $f_{uv}^l = f_{uv} = f_{uv}^u$ for all $(u, v) \in E$. Then, the summed weights of the paths are equal to the summed flow values of all outgoing edges of s (the complete $s - t$ -flow value) and build both a lower and upper bound on $\sum_{i=1}^{\bar{K}} w_i$. Consequently, finding a minimum flow decomposition, which is NP-hard [VCCM08], minimizes the objective. \square

The opposite is the case if $a_y = 0$ and $a_w > 0$. To show this, we first revisit the *minimum-cost flow problem* [Orl88] in capacitated networks.

Definition 10 (Minimum-cost flow problem [Orl88]). *Given a tuple $G(V, E, d, c)$, where $G(V, E)$ is a digraph, $d(v) \in \mathbb{Z}$ represents the demand ($d(v) \leq 0$) or the supply ($d(v) > 0$) of node $v \in V$ and $c(u, v) \geq 0$ is the cost associated with every edge $(u, v) \in E$. The minimum-cost flow problem (MCFP) is to find a flow $f \in \mathbb{N}_{\geq 0}^{|E|}$ with minimum cost $\sum_{(u,v) \in E} c(u, v) \cdot f_{uv}$ such that*

$$\sum_{u:(u,v) \in E} f_{uv} - \sum_{w:(v,w) \in E} f_{vw} = d(v) \quad (16)$$

is satisfied for all $v \in V$. In capacitated networks, we have $G(V, E, d, c, f, \bar{f})$ with lower f_{uv} and upper bounds \bar{f}_{uv} on the flow f_{uv} associated with each edge $(u, v) \in E$, which also have to be fulfilled.

Lemma 11. *For $a_y = 0$ and $a_w > 0$, MWIFDP can be solved in polynomial time.*

Proof. This particular case can be reduced to the minimum-cost flow problem in capacitated networks, which can be solved in polynomial time [Orl88, Way99, ZYGDD11]. For a given inexact flow network $G(V, E, f^l, f^u)$, we show that solving the MWIFDP with $a_y = 0$ and $a_w > 0$ corresponds to finding a minimal cost flow in the following graph.

For $G'(V', E', d, c, f, \bar{f})$, let $V' = V \cup \{s'\} \cup \{t'\}$ be the node set with a super-source s' and super-sink t' and $E' = E \cup \{(s', s), (t, t'), (s', t')\}$ the corresponding edges. We set the supply and demand of s' and t' equal to the summed upper bounds on the flow values $\sum_{(u,v) \in E} f_{uv}^u =: M$, i.e., $d(s') = M = -d(t')$, while we have $d(v) = 0$ for all other nodes $v \in V$. For the cost function c , we have $c(s', s) = 1$ and

$c(e) = 0$ for all $e \in E' \setminus \{(s', s)\}$, and the lower and upper bounds, \underline{f}, \bar{f} , on the flow are defined as $(\underline{f}_{uv}, \bar{f}_{uv}) := (f_{uv}^l, f_{uv}^u)$ for $(u, v) \in E$ and $(\underline{f}_{uv}, \bar{f}_{uv}) := (0, M)$ for $(u, v) \in \{(s', s), (t, t'), (s', t')\}$.

In other words, we extend the original graph $G(V, E, f^l, f^u)$ so that all flow units required to fulfill the constraints on the bounds f^l and f^u have to use edge (s', s) at a cost of 1 each. The remaining flow can use the edge (s', t') with a cost of 0. An illustration of $G'(V', E', d, c, \underline{f}, \bar{f})$ can be found in Figure 2.

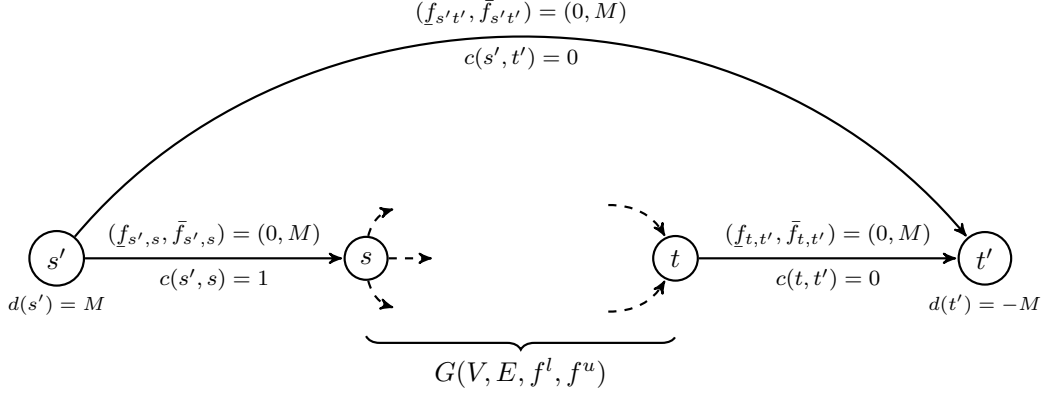


Figure 2: Illustration of transformed graph $G'(V', E', d, c, \underline{f}, \bar{f})$ for the MCFP to solve the MWIFDP for $a_y = 0$ and $a_w > 0$ in $G(V, E, f^l, f^u)$.

If we now consider a minimum cost flow f^m in $G'(V', E', d, c, \underline{f}, \bar{f})$, we can construct a feasible flow f for the MWIFDP in the original graph $G(V, E, f^l, f^u)$ by removing edges $(s', s), (t, t'), (s', t')$ with corresponding flow values. That means we have a flow $f \in \mathbb{N}_{\geq 0}^{|E|}$ with $f_{uv} := f_{uv}^m$ for $(u, v) \in E$ that is a feasible solution for MWIFDP by fulfilling the same flow and bound constraints. Since each flow unit in f traverses edge (s', s) with cost 1, the total flow value equals the flow cost $c(f^m) := \sum_{(u,v) \in E'} c(u, v) \cdot f_{uv}^m = f_{s's}^m$ and is therefore minimal. Due to the fact that the number of $s - t$ -paths can be arbitrarily large without affecting the objective function and we can easily decompose f into $c(f^m)$ $s - t$ -paths each with weight 1, and this minimizes $a_w \sum_{i=1}^K w_i = a_w c(f^m)$ in (15). \square

Lemma 12. *For $a_y = 0$ and $a_w > 0$, the strictly robust counterpart of MWIFDP with uncertainty sets \mathcal{U} and $\mathcal{U}(\Gamma)$ in Section 3.3 can be solved in polynomial time.*

Proof. Using the same reasoning as in Section 3.3, we can reduce the uncertain optimization problem of MWIFDP to solving MWIFDP for the respective worst-case scenario for \mathcal{U} and $\mathcal{U}(\Gamma)$. Consequently, we use the procedure in Lemma 11 with $(\underline{f}_{uv}, \bar{f}_{uv}) = (\bar{f}_{uv}^l, \underline{f}_{uv}^u)$ and $(\underline{f}_{uv}, \bar{f}_{uv}) = (\min\{\hat{f}_{uv}^l + \Gamma, \bar{f}_{uv}^l\}, \max\{\hat{f}_{uv}^u - \Gamma, \underline{f}_{uv}^u\})$ for all $(u, v) \in E$ regarding the uncertainty sets \mathcal{U} and $\mathcal{U}(\Gamma)$, respectively. \square

4.2 Formulation without upper bounds

Now, for the remainder of this section, we neglect the upper bounds on the flow, i.e., we consider (15) without constraints (15f). This allows us to give some interesting complexity results for both the nominal case and the strictly robust counterpart of different variants.

Let \mathcal{U} be an interval-wise uncertainty set with

$$\mathcal{U} = \left\{ f^l \in \mathbb{N}_{\geq 0}^{|E|} : f_{uv}^l \in [\underline{f}_{uv}^l, \bar{f}_{uv}^l], \forall (u, v) \in E \right\}, \quad (17)$$

for given $\underline{f}^l, \bar{f}^l \in \mathbb{N}_{\geq 0}^{|E|}$ and $\mathcal{U}(\Gamma)$ the corresponding Γ -uncertainty set with

$$\mathcal{U}(\Gamma) = \left\{ f^l \in \mathbb{N}_{\geq 0}^{|E|} : f_{uv}^l \in [\underline{f}_{uv}^l, \bar{f}_{uv}^l], \forall (u, v) \in E; \sum_{(u,v) \in E} |f_{uv}^l - \underline{f}_{uv}^l| \leq \Gamma \right\}. \quad (18)$$

for a given uncertainty budget $\Gamma \in \mathbb{R}_{\geq 0}$ and nominal case $\hat{f} = \underline{f}^l$. We can assume w.l.o.g. that $\Gamma \in \mathbb{N}_{\geq 0}$ since $f^l \in \mathbb{N}_{\geq 0}^{|E|}$. The idea behind $\mathcal{U}(\Gamma)$ is that, in many cases, it is reasonable to assume that the flow values f_{uv}^l do not attain their maximum in the interval $[\underline{f}_{uv}^l, \bar{f}_{uv}^l]$ on all edges $(u, v) \in E$ simultaneously. To reflect this, the cumulative deviation from the nominal scenario can be limited with the help of Γ .

Now, we can adopt the reasoning in Lemma 6 and Lemma 7 in Section 3.3 for the lower bounds. Consequently, a worst-case scenario in the strictly robust case is \bar{f}_{uv}^l and $\min\{\hat{f}_{uv}^l + \Gamma, \bar{f}_{uv}^l\}$ for all $(u, v) \in E$ regarding \mathcal{U} and $\mathcal{U}(\Gamma)$, respectively.

Moreover, one can notice that Lemma 12 also holds for this modified version of MWIFDP without upper bounds.

Lemma 13. *For $a_y = 0$ and $a_w > 0$, the strictly robust counterpart of MWIFDP without upper bounds and with uncertainty sets \mathcal{U} in (17) and $\mathcal{U}(\Gamma)$ in (18) can be solved in polynomial time.*

Proof. We follow the proof of Lemma 12, but since we have no upper bounds, we set them to ∞ for the MCFP. That means we have $(\underline{f}_{uv}, \bar{f}_{uv}) = (f_{uv}^l, \infty)$ concerning uncertainty set \mathcal{U} and $(\underline{f}_{uv}, \bar{f}_{uv}) = (\min\{\hat{f}_{uv}^l + \Gamma, \bar{f}_{uv}^l\}, \infty)$ concerning $\mathcal{U}(\Gamma)$.

Consequently, the same reasoning also applies here: Since the flow constraints have to be satisfied and the lower bound for each $(u, v) \in E$ is \underline{f}_{uv} , each edge (with $\underline{f}_{uv} > 0$) is covered by one or more paths with a summed weight of at least \underline{f}_{uv} . Due to the fact that each $s - t$ -path is a $s' - t'$ path that uses edge (s', s) with $c(s, s') = 1$, the summed weights of all $s - t$ -paths are minimized.

Instead of ∞ , we can use a sufficiently large value (e.g., $\sum_{(u,v) \in E} \underline{f}_{uv}$) as an upper bound. \square

Surprisingly, if we consider the alternative case with $a_y > 0$ and $a_w = 0$, i.e., the MIFDP without upper bounds, we obtain a different complexity result than in Section 4.1.

Lemma 14. *For $a_y > 0$ and $a_w = 0$, the strictly robust counterpart of MWIFDP without upper bounds and with uncertainty sets \mathcal{U} in (17) and $\mathcal{U}(\Gamma)$ in (18) can be solved in polynomial time.*

Proof. Due to the fact that the weights w_i can be arbitrarily large without affecting the objective function, we can choose

$$w_i := \sum_{(u,v) \in E} \bar{f}_{uv}^l$$

for $i = 1, \dots, \bar{K}$, which is feasible for every realization of f^l . Now, the problem reduces to finding a minimal number of $s - t$ -paths covering all edges with $\bar{f}_{uv}^l > 0$ ($\min\{\hat{f}_{uv}^l + \Gamma, \bar{f}_{uv}^l\} > 0$) in the strictly robust case regarding the uncertainty set \mathcal{U} ($\mathcal{U}(\Gamma)$).

Once again, we can use the proof of Lemma 11 to show that this corresponds to finding a minimal cost flow. However, there is a modification that is required for the lower bounds \underline{f} , as we only want to cover the edges that have a positive flow in the corresponding worst-case scenario. Therefore, it is sufficient to set 1 as the lower bound for these. Consequently, we have $(\underline{f}_{uv}, \bar{f}_{uv}) := (1, \infty)$ for all $(u, v) \in E$ with $\bar{f}_{uv}^l > 0$ and $(\underline{f}_{uv}, \bar{f}_{uv}) := (0, \infty)$ for $(u, v) \in \{(s', s), (t, t'), (s', t')\} \cup \{(u, v) \in E : \bar{f}_{uv}^l = 0\}$ in the strict robust case. For the Γ -uncertainty set $\mathcal{U}(\Gamma)$, we have $(\underline{f}_{uv}, \bar{f}_{uv}) := (1, \infty)$ for all $(u, v) \in E$ with $\min\{\hat{f}_{uv}^l + \Gamma, \bar{f}_{uv}^l\} > 0$ and $(\underline{f}_{uv}, \bar{f}_{uv}) := (0, \infty)$ for $(u, v) \in \{(s', s), (t, t'), (s', t')\} \cup \{(u, v) \in E : \min\{\hat{f}_{uv}^l + \Gamma, \bar{f}_{uv}^l\} = 0\}$. Note that this is independent of Γ if $\Gamma > 0$, as the set $\{(u, v) \in E : \min\{\hat{f}_{uv}^l + \Gamma, \bar{f}_{uv}^l\} = 0\}$ is then always empty.

Considering an optimal minimum-cost flow in this modified graph, each relevant edge is covered by at least one $s' - t'$ -path (and thus $s - t$ -path), while the first edge of each $s' - t'$ path has cost 1. Consequently, we minimize the number of $s - t$ -paths covering all relevant edges. \square

5 Adjustable robust flow decomposition

As we have seen in the previous sections, even if we know that the uncertainty set is restricted and only a few edges in each scenario have a positive flow, we still need to set weights that cover all edges that have a positive flow in any scenario. As a result, the number of paths (and the sum of weights) in the solution is much larger than what is actually required for any realized scenario. Moreover, the uncertainty set must allow for a solution that is feasible for all scenarios. To overcome the rigidity of

the solutions obtained by the strictly robust model, we make use of adjustable robustness, introduced in Section 3.2 to allow part of the decisions to be made after the uncertainty has been observed.

Depending on the application at hand, it may be essential to know the number of paths a priori or to specify a superset of paths from which to choose. Considering the field of transportation, we can have a situation where we need to know beforehand how many vehicles (corresponding to the number of paths y) will be required but can decide on capacities (w) and routes (x) later, as well as a situation where both the routes (x) and the number of drivers (y) must be known in advance, but the vehicles with suitable capacities (w) can be selected depending on the final realization.

As we can make three different types of decisions (number of paths, paths, weights) corresponding to the three different variable types (y, x, w), this naturally results in two adjustable robust optimization versions of MWIFDP based on (15). In the first formulation, we have one here-and-now and two wait-and-see decisions, i.e., we first make a decision on the number of paths y and then decide on the paths x and weights w depending on the observed scenario ξ . Since we only have one set of non-adjustable variables, we call it the more adjustable formulation MA . Consequently, in the second less adjustable formulation, denoted by LA , we first make a decision on the routes (x) and how many of them (y), and then we decide on the weights (w) depending on the scenario ξ . An overview of both adjustable formulations can be found in Table 1.

	MA (more adjustable formulation)	LA (less adjustable formulation)
a priori	number of paths	number of paths, paths
a posteriori	paths, weights	weights
non-adjustable	y	y, x
adjustable	x, w	w
solution method	Algorithm 1	Algorithm 3
models	MIP formulation (19), master problem (20), sub-problem (21)	MIP formulation (22), master problem (23), sub-problem (24)
	<ul style="list-style-type: none"> • results in a lower number of paths • depending on the scenario, different paths might be used 	<ul style="list-style-type: none"> • results in a smaller pool of paths covering all scenarios

Table 1: Overview of both adjustable formulations.

For MA , the resulting MIP formulation can be found in (19). The adjustable variables x^ξ and w^ξ now depend on the scenario $\xi \in \mathcal{U}$ (given by the bounds $f^{l,\xi}$ and $f^{u,\xi}$) and, as a consequence, the sum of weights are moved to the constraints (19b) and substituted by variable \mathcal{W} in the objective function.

$$\min_{x, y, w} \sum_{i=1}^{\bar{K}} y_i + \mathcal{W} \quad (19a)$$

$$\text{s.t.} \quad \sum_{i=1}^{\bar{K}} w_i^\xi \leq \mathcal{W}, \quad \forall \xi \in \mathcal{U}, \quad (19b)$$

$$\sum_{v:(s,v) \in E} x_{svi}^\xi = y_i, \quad \forall i \in \{1, \dots, \bar{K}\}, \xi \in \mathcal{U}, \quad (19c)$$

$$\sum_{u:(u,t) \in E} x_{uti}^\xi = y_i, \quad \forall i \in \{1, \dots, \bar{K}\}, \xi \in \mathcal{U}, \quad (19d)$$

$$\sum_{(u,v) \in E} x_{uvi}^\xi - \sum_{(v,w) \in E} x_{vwi}^\xi = 0, \quad \forall i \in \{1, \dots, \bar{K}\}, v \in V \setminus \{s, t\}, \xi \in \mathcal{U}, \quad (19e)$$

$$\sum_{i \in \{1, \dots, \bar{K}\}} w_i^\xi x_{uvi}^\xi \geq f_{uv}^{l,\xi}, \quad \forall (u, v) \in E, \xi \in \mathcal{U}, \quad (19f)$$

$$\sum_{i \in \{1, \dots, \bar{K}\}} w_i^\xi x_{uvi}^\xi \leq f_{uv}^{u,\xi}, \quad \forall (u, v) \in E, \xi \in \mathcal{U}, \quad (19g)$$

$$\mathcal{W} \in \mathbb{Z}^+, \quad (19h)$$

$$w_i^\xi \in \mathbb{Z}^+, \quad \forall i \in \{1, \dots, \bar{K}\}, \xi \in \mathcal{U}, \quad (19i)$$

$$x_{uvi}^\xi \in \{0, 1\}, \quad \forall (u, v) \in E, i \in \{1, \dots, \bar{K}\}, \xi \in \mathcal{U}, \quad (19j)$$

$$y_i \in \{0, 1\}, \quad \forall i \in \{1, \dots, \bar{K}\}. \quad (19k)$$

For LA , we have a similar formulation, with the key difference being that only the variables w^ξ are adjustable. This can be found in (22) in Appendix A.2.

Lemma 15. *The objective value of the optimal solution to MA in (19) is less or equal to the objective value of the optimal solution to LA in (22).*

Proof. We show that all feasible solutions to LA in (22) are also feasible to MA in (19) and have the same objective value. Let $(\check{y}, \check{x}, \check{w})$ be a feasible solution to LA with

$$(\check{y}, \check{x}, \check{w}) = (\check{y}_i, \check{x}_{uvi}, \check{w}_i^\xi)_{(u,v) \in E, i \in \{1, \dots, \bar{K}\}, \xi \in \mathcal{U}}.$$

Since both formulations (22) and (19) differ only in the variable x ((22j) and (19j)), we construct a solution $(\dot{y}, \dot{x}, \dot{w})$ with

$$(\dot{y}, \dot{x}, \dot{w}) = (\dot{y}_i, \dot{x}_{uvi}^\xi, \dot{w}_i^\xi)_{(u,v) \in E, i \in \{1, \dots, \bar{K}\}, \xi \in \mathcal{U}}.$$

to MA as follows. We set

$$\begin{aligned} \dot{y}_i &:= \check{y}_i, & \forall i \in \{1, \dots, \bar{K}\}, \\ \dot{w}_i^\xi &:= \check{w}_i^\xi, & \forall i \in \{1, \dots, \bar{K}\}, \xi \in \mathcal{U}, \\ \dot{x}_{uvi}^\xi &:= \check{x}_{uvi}, & \forall (u, v) \in E, i \in \{1, \dots, \bar{K}\}, \xi \in \mathcal{U}, \end{aligned}$$

whereby the latter is feasible because \check{x} satisfies constraints (22c)-(22g) for all scenarios $\xi \in \mathcal{U}$, and thus, \dot{x} also fulfills constraints (19c)-(19g). It is easy to see that the objective value has not changed, which completes the proof.

Note that this does not apply vice versa, as here the variables x depend on scenario $\xi \in \mathcal{U}$ and are therefore generally not feasible for all scenarios. \square

In contrast to strict robustness, an edge e for which the intersection of the intervals $[f_e^{l,\xi}, f_e^{u,\xi}]$ of all scenarios ξ is empty no longer automatically implies infeasibility. As a result, the discrete uncertainty set in (11) is not necessarily reduced to an interval-wise uncertainty set.

Naturally, (19) and (22) reduce to the MWIFDP formulation in (15) if we only have one scenario, but unlike the interval-wise uncertainty set, with discrete uncertainty set (11) we need to consider more than one scenario in the general case.

The MIP formulations (19) and (22) yield challenging problems with steep, impractical computational requirements. Therefore, to solve the proposed adjustable variants *LA* and *MA*, we adapt the *column-and-constraint generation* approach in [ZZ13] to find a minimal subset $\bar{\mathcal{U}}$ of \mathcal{U} that is sufficient to *cover* the adjustable problem for the complete uncertainty set \mathcal{U} . Here, we say that $\bar{\mathcal{U}} \subset \mathcal{U}$ *covers* \mathcal{U} if solving the problem for $\bar{\mathcal{U}}$ returns the same solution as solving the problem for \mathcal{U} . The adaption relates to the fact that, while in [ZZ13] the uncertainty set \mathcal{U} is assumed to be continuous (with a finite number of extreme points and rays), our uncertainty set is discrete and finite. Nevertheless, the convergence result in [ZZ13] still guarantees that the proposed column-and-constraint generation algorithm will converge and return an optimal solution for a set $\bar{\mathcal{U}}$ that covers \mathcal{U} .

Therefore, we start by solving formulation (19) (or (22)) with subset $\bar{\mathcal{U}}$ that includes initially one arbitrary scenario. This is the so-called *master problem*. We use the resulting solution of the non-adjustable variables to fix them in the *sub-problem*, where we then solve the formulation for all scenarios $\xi \in \mathcal{U}$. The scenario ξ^* with the highest solution value or that causes infeasibility is added to $\bar{\mathcal{U}}$ and the steps are repeated until the solution value of the master problem equals the solution value of the sub-problem (in particular, it is feasible for all scenarios). For *MA*, a detailed description of the column-and-constraint generation method can be found in Algorithm 1 and the corresponding formulations of the master problem and sub-problem in (20) and (21) in Appendix A.1. If a given solution (y^k) for the master problem leads to an infeasible sub-problem, we know that we need at least one more path. As a consequence, in line 13 of Algorithm 1, we add the corresponding constraint to the master problem (20). If this is the case in *LA*, we only know that the combination of (y^k) and (x^k) causes infeasibility of the sub-problem. Therefore, we add the constraint

$$\sum_{i:(y^k)_i=0} y_i + \sum_{i:(x^k)_i=0} x_i + \sum_{i:(y^k)_i=1} (1 - y_i) + \sum_{i:(x^k)_i=1} (1 - x_i) \geq 1$$

to the master problem (23) to eliminate this combination. This can be found in Appendix A.2 in Algorithm 3 with the corresponding formulations of the master problem and sub-problem of *LA* in (23) and (24).

Algorithm 1: Column-and-constraint generation method for *MA*

```

1 given a scenario set  $\mathcal{U}$  and threshold  $\epsilon$ ;
2 set  $LB = -\infty$ ,  $UB = \infty$ ,  $k = 1$  and initialize  $\bar{\mathcal{U}}$  with one scenario from  $\mathcal{U}$ ;
3 while  $UB - LB > \epsilon$  do
4   solve master problem (20), get optimal solution  $(y^k, x^k, w^k, \mathcal{W}^k)$ ;
5   update lower bound  $LB = \sum_{i=1}^{\bar{K}} (y^k)_i + \mathcal{W}^k$ ;
6   solve sub-problem (21) with input  $(y^k)$ ;
7   if we get optimal solution  $(\bar{x}^k, \bar{w}^k, \bar{\mathcal{W}}^k)$  then
8     let  $\xi^k$  be the worst-case scenario causing  $\bar{\mathcal{W}}^k$ ;
9     update upper bound  $UB = \sum_{i=1}^{\bar{K}} (y^k)_i + \bar{\mathcal{W}}^k$ ;
10  end
11  else
12    let  $\xi^k$  be the first scenario causing infeasibility;
13    add  $\sum_{i=1}^{\bar{K}} y_i \geq \sum_{i=1}^{\bar{K}} (y^k)_i + 1$  to constraints of master problem (20);
14  end
15  add  $\xi^k$  to  $\bar{\mathcal{U}}$ ;
16   $k = k + 1$ ;
17 end
18 return  $(y^k, \bar{x}^k, \bar{w}^k)$ ;

```

Even though it may be necessary in theory to consider all scenarios in the master problem, a much smaller number is sufficient in most cases, as we see in the experimental evaluation in Section 6.

To evaluate the aforementioned adjustable formulations, we add a third conservative method, the so-called *naive approach*. Here, we solve the problem for each scenario separately and then add all paths with corresponding weights to a set of paths. If solutions for different scenarios use the same

path, we add the path only once. To calculate \mathcal{W} , we use the maximum of the summed weights of the scenarios. Consequently, this is a heuristic solution for LA , giving us an upper bound on LA and, thus, also on MA .

6 Computational study

In this section, we experimentally evaluate both adjustable robust optimization versions of the MWIFDP introduced in the previous Section 5 to quantify the benefit of adaptability when taking into account the uncertainty. Moreover, we show that both MA and LA considerably outperform the naive approach, in which we solve the problem for each scenario separately. As described in the previous section, we use the column-and-constraint generation methods in Algorithm 1 and Algorithm 3 as solution methods.

6.1 Data and scenarios

Due to this being the first work to consider the MWIFDP and additionally adjustable robustness, we could not find instances in the literature that we could use directly for our purposes. Therefore, we adapt graph-structured instances from the literature that are related to our work both theoretically and practically. As mentioned in Section 1, the most recent references concerning MFD comes from the field of bioinformatics, providing many datasets for the application of RNA transcript assembly. Here, we select two of the instances also used in [DWM22] and [DT23], both being acyclic splice graphs, one for a human gene and one for a mouse gene. Additionally, we add a benchmark instance for a minimum-cost flow problem from [Vel93] denoted by *gte* and a graph that contains regional railway data of Lower Saxony, a region in northern Germany. The latter comes from the scientific software toolbox LinTim [SSJ+24], which deals with solving various planning steps in public transport. Since this is not originally an $s-t$ -flow network, we modified it by adding 71 auxiliary edges for all missing outgoing edges of s and incoming edges of t . To complement this, we also use the artificial graph from Example 4 in Section 3.1, which also comes from [DT23]. A description of all instances can be found in Table 2 and the corresponding plots in Figure 1a and Figure 3.

id	name	#nodes	#edges	s	t	origin	plot
1	small	7	12	0	6	Example 4	Figure 1a
2	lowersaxony	36	103	0	35	[SSJ+24]	Figure 3a
3	human	24	39	0	23	[DWM22, DT23]	Figure 3b
4	mouse	111	120	0	110	[DWM22, DT23]	Figure 3c
5	gte	49	130	4	17	[Vel93]	Figure 3d

Table 2: Graph properties of the original instances.

Scenario generation Deriving meaningful scenarios for the aforementioned instances is more challenging than one might expect. Besides the fact that each scenario must be feasible on its own, the difficulty lies in ensuring that the uncertainty set $\mathcal{U}(\Gamma)$ is sufficiently diverse to provide required protection levels whilst not being so disparate that they become unrealistic or impractical, rendering any robust consideration senseless.

To generate the scenarios that form the uncertainty set, we sample a random subset \mathcal{P}' of $s-t$ -paths of size $p := |\mathcal{P}'|$ in the graph and set the flow value of each edge $e \in E$ to the number of occurrences of e in these $s-t$ -paths. Consequently, \mathcal{P}' , with associated path weights all equal to 1, forms a $|\mathcal{P}'|$ -flow decomposition for the constructed flow network with weight $|\mathcal{P}'|$. That means we guarantee feasibility and control the ratio of summed weights to be the number of paths since both are highly correlated and bounded by the subset size $|\mathcal{P}'|$. We then define lower and upper bounds around these flow values for each edge $e \in E$ to construct one scenario. Since we sample a new subset \mathcal{P}' of $s-t$ -paths for each scenario, this provides the uncertainty set with a reasonable variety of scenarios.

In order to measure and eliminate highly divergent scenarios from the uncertainty set, we first construct a nominal scenario $(f_{uv}^*, f_{uv}^{l,*}, f_{uv}^{u,*}, (u,v) \in E)$ using this method and then only include scenarios whose summed deviations lie within a certain range Γ of the nominal scenario. The detailed

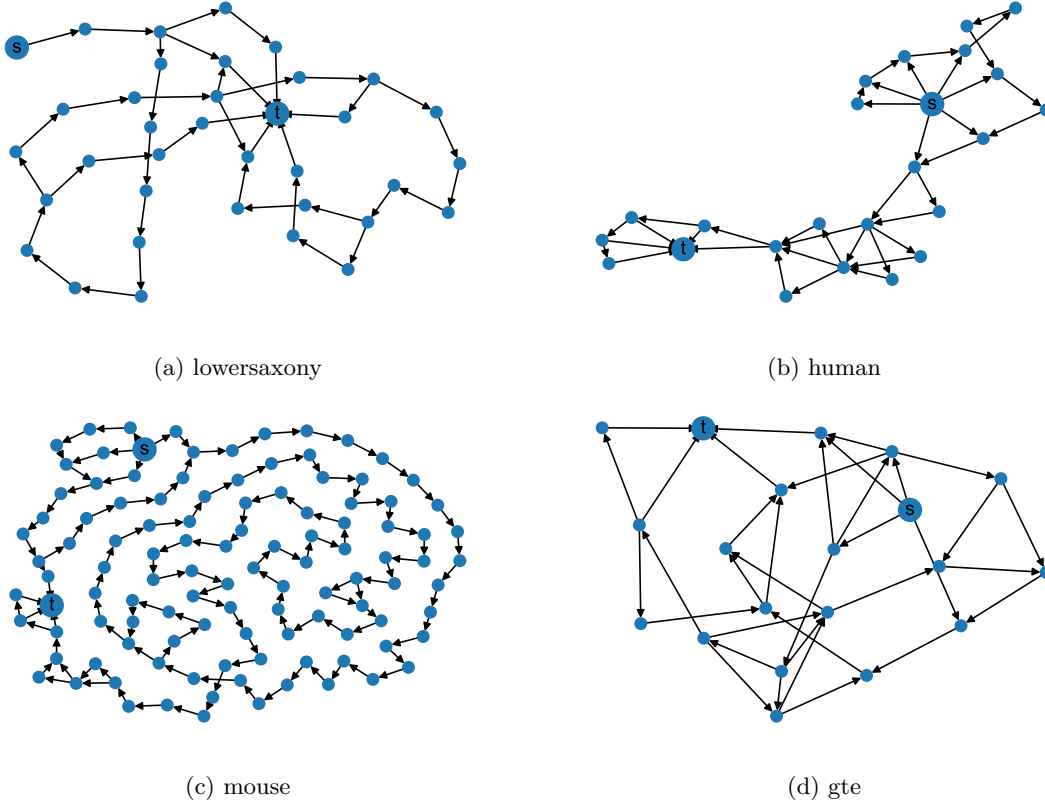


Figure 3: Graph structures of the original instances.

procedure is outlined in Algorithm 2. Since in our computations, subset sizes $|\mathcal{P}'|$ of value 5, 10, and 20 produce very similar results, we use $|\mathcal{P}'| = 10$ in what follows.

To define the range around the flow values for the lower and upper bounds, we use $\delta = \frac{|\mathcal{P}'|}{2}$. Note that f_{uv} is bounded by $|\mathcal{P}'|$. Due to the size of the graphs, f_{uv} is closer to 0 in most cases, which is why we draw the lower bound in the interval $[\max(0, f_{uv} - 2), f_{uv}]$ for all $(u, v) \in E$. Note that all auxiliary edges have a lower bound of zero, so they never need to be covered but can always be used if required. Accordingly, we set the lower bounds $f_{uv}^{l,*}$ and $f_{uv}^{l,\xi}$ for the *lowersaxony* instance to 0 if $u = s$ or $v = t$ (auxiliary edges).

6.2 Experimental results

As mentioned in the previous section, we choose subset size $|\mathcal{P}'| = 10$. For Γ' , we use 0.1, 0.2, and 0.3, i.e., the allowed summed deviations to the nominal scenario lie within a range of 10 %, 20 %, and 30 %, respectively. As for the uncertainty set sizes, we use $|\mathcal{U}(\Gamma)| = 5, 10, 50, 100, 200, 500$ since the differences in the results become smaller for the larger sizes. Due to the complexity of the problem, we set a time limit of 24 hours for executing the complete algorithm while ensuring full iterations of the master problem and sub-problem. This means if the time limit is not reached after solving one of both problems, we do not interrupt the computation of the following problem, even if the time limit is exceeded in the meantime. We set a time limit of 30 minutes for the master problem. If no feasible solution is obtained within this time, the calculation continues until one is found. For the sub-problem, it is sufficient to limit the time to 3 minutes. Here, we take advantage of the fact that it can be solved individually for each scenario instead of considering them all at once. This significantly reduces the computational burden, but it also means that the solution time of the sub-problem scales with the number of scenarios, as they are solved sequentially (this could be overcome by parallelization). For the naive approach, we use a maximum of one hour per scenario.

As already indicated, the adjustable version of MWIFDP is computationally challenging, which

Algorithm 2: Description of scenario generation

```
1 given digraph  $G(V, E)$ : compute all  $s - t$ -paths  $\mathcal{P}(G)$  and set  $\mathcal{U}(\Gamma) = \emptyset$ ,  $\delta = \frac{p}{2}$ ;  
2 initialize  $f_{uv}^* = 0$  for all  $(u, v) \in E$ ; // nominal scenario  
3 sample a random subset of paths  $\mathcal{P}' \subset \mathcal{P}(G)$  with size  $|\mathcal{P}'| = p$ ;  
4 update  $f_{uv}^* = f_{uv}^* + 1$  for all  $(u, v) \in P$  for each path  $P \in \mathcal{P}'$ ;  
5 set  $f_{uv}^{l,*} = f_{uv}^*$  and  $f_{uv}^{u,*} = f_{uv}^* + \delta$  for all  $(u, v) \in E$ ;  
6  $\xi = 1$ ; // other scenarios  
7 while  $|\mathcal{U}(\Gamma)| < \text{required number of scenarios}$  do  
8   initialize  $f_{uv} = 0$  for all  $(u, v) \in E$ ;  
9   sample a random subset of paths  $\mathcal{P}' \subset \mathcal{P}(G)$  with size  $|\mathcal{P}'| = p$ ;  
10  update  $f_{uv} = f_{uv} + 1$  for all  $(u, v) \in P$  for each path  $P \in \mathcal{P}'$ ;  
11  draw  $f_{uv}^{l,\xi} \in [\max(0, f_{uv} - 2), f_{uv}]$  and set  $f_{uv}^{u,\xi} = f_{uv} + \delta$  for all  $(u, v) \in E$ ;  
12  if  $\sum_{e \in E} |f_e^{l,\xi} - f_e^{l,*}| + |f_e^{u,\xi} - f_e^{u,*}| \leq \Gamma' \cdot \sum_{e \in E} (f_e^{l,*} + f_e^{u,*}) =: \Gamma$  then  
13    add scenario  $(f^{l,\xi}, f^{u,\xi})$  to uncertainty set  $\mathcal{U}(\Gamma)$ ;  
14    update  $\xi = \xi + 1$ ;  
15  end  
16 end  
17 return  $\mathcal{U}(\Gamma)$ ;
```

model	small	lowersaxony	human	mouse	gte
<i>MA</i>	382.56	6200.08	3687.06	78.04	11289.26
<i>LA</i>	52873.67	47353.45	60309.20	84434.52	66440.38
naive	788.61	1817.98	2481.08	831.86	3825.67

Table 3: Runtimes for the different formulations and instances in seconds, averaged over all uncertainty set sizes and values for Γ' .

is why we use the column-and-constraint generation method. Indeed, the master problem alone, consisting of an adjustable MWIFDP (with a reduced number of scenarios that increases as iterations progress), is in itself computationally demanding. While in *MA*, there is only one set of non-adjustable variables, and thus x and w can be chosen individually depending on the scenario, in *LA*, both y and x must be feasible (and in the best case optimal) for all scenarios. This leads to the less adjustable formulation *LA* being significantly harder to solve, which is reflected in the runtimes and number of iterations found in Table 3 and Table 4, respectively. The numbers provided refer to the average of all uncertainty set sizes $|\mathcal{U}(\Gamma)|$ and values for Γ' . Note that we use a pre-solving phase to initialize the value for the lower bound, which we do not count in the number of iterations. More precisely, after initializing $|\mathcal{U}(\Gamma)|$, we solve the master problem without upper bounds on the flow values and also without \mathcal{W} in the objective function (corresponding to Lemma 14). The resulting value for the number of paths is used to initialize *LB*.

model	small	lowersaxony	human	mouse	gte
<i>MA</i>	2.00	4.72	1.72	1.17	2.94
<i>LA</i>	31.33	30.39	30.22	39.95	36.44

Table 4: Iterations for the different formulations and instances, averaged over all uncertainty set sizes and values for Γ' .

While *MA* rarely reaches the time limit and usually requires only a few iterations to converge, the opposite is true for *LA*. The particularly low mean runtimes of *MA* for *small* and *mouse* can be explained by the small graph size and simple structure of the graph (very long paths without branches), respectively. For *LA*, however, these are dominated by the additional complexity incurred by the less adjustable master problem. Moreover, the fact that with *MA*, we have two adjustable variable sets causes the sub-problem to no longer be solved in a few seconds, as with *LA*, where only the optimal

values for w need to be computed. However, since we can consider the sub-problem individually for each scenario, the computational requirements are still moderate. Nevertheless, the fact that we do not solve the scenarios in parallel means that the runtime for *MA* can be significantly longer for larger uncertainty set sizes. As a consequence, the results discussed below are not necessarily optimal.

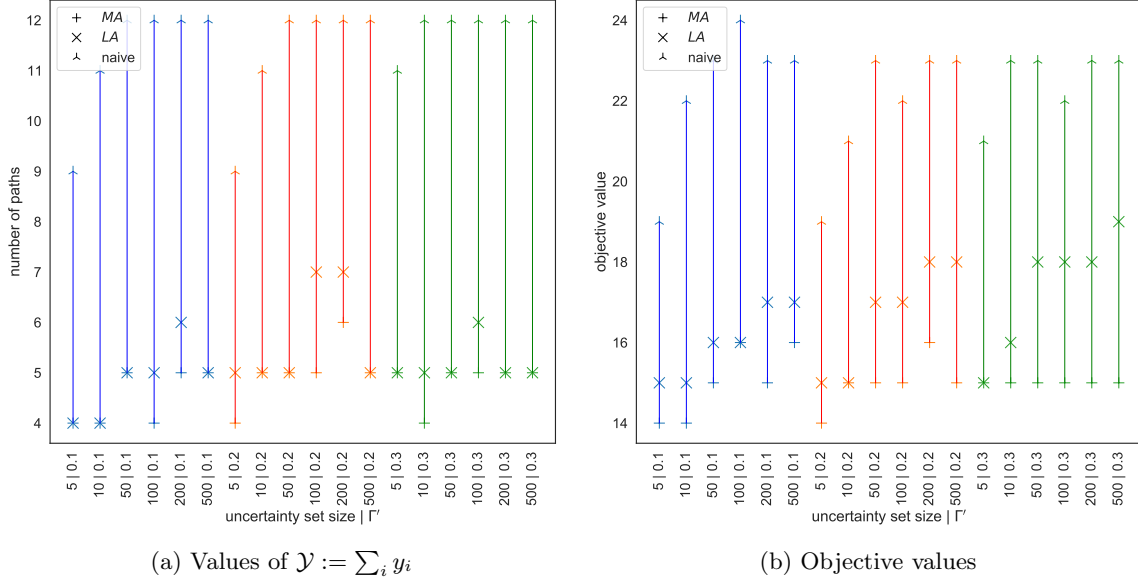


Figure 4: Results of *MA*, *LA* and the naive approach for instance set *small* for the different uncertainty set sizes $|\mathcal{U}(\Gamma)|$ and values for Γ' .

For the sake of clarity, we only show detailed results for the instance sets *small*, *lowersaxony*, and *human*. All other results can be found in Appendix B. For *small*, Figure 4 shows both the values for $\sum_i y_i := \mathcal{Y}$ and the objective values for the different uncertainty set sizes and values for Γ . The objective values for *lowersaxony* and *human* are shown in Figures 5a and 5b, respectively. As we can see, the values for *MA* are consistently the lowest and those of the naive approach the highest. This also aligns with theoretical reasoning, which states that the less adjustable formulation *LA* can never achieve better objective values than *MA* and is bounded from above by the objective function value of the naive approach. These theoretical properties apply to the objective value but not necessarily to the number of paths. Nevertheless, the experimental results also show the same behavior for the latter.

Since we use a set of $s - t$ -paths of size $|\mathcal{P}'|$ to create a scenario, we know that we can decompose each scenario into a maximum of $|\mathcal{P}'|$ $s - t$ -paths. This means that in *MA*, $\sum_i y_i$ is bounded by $|\mathcal{P}'|$ since we only have to determine the maximum number of paths that is sufficient per scenario. For *LA*, in addition to the number, the paths themselves must also be specified, forming a feasible solution for all scenarios. Consequently, the union of the original $s - t$ -paths of all scenarios is feasible, i.e., $\sum_i y_i$ is bounded by $|\mathcal{U}(\Gamma)| \cdot |\mathcal{P}'|$. With this theoretical background, however, it can be seen from the results that these bounds are not even close to being reached. Depending on the instance, the maximum number of paths ranges between 5 and 8 for *MA*, 7 and 19 for *LA*, and 12 to 652 for the naive approach, while the theoretical upper bound is 5000.

In terms of the summed weights \mathcal{W} , the results of *MA* and the naive approach are similar (between 6 and 12) and hardly vary for different values of $|\mathcal{U}(\Gamma)|$ and Γ' . This can be explained by the fact that with both methods, the paths and weights can be adjusted to each other and chosen to suit the scenario. In contrast, *LA* searches for a set of paths that fits all scenarios. Consequently, it becomes harder to match the paths with the different values for w to the individual scenario, which leads to significantly higher values of \mathcal{Y} and \mathcal{W} (between 6 and 21) and also to both increasing with growing $|\mathcal{U}(\Gamma)|$ and Γ' .

When looking at \mathcal{Y} , we see a similar picture for *MA* as we did before with \mathcal{W} . Due to the more comprehensive adjustability, the values are relatively small (between 3 and 8), and the increase with growing $|\mathcal{U}(\Gamma)|$ and Γ' is also modest. The opposite is the case with the naive approach. Since the

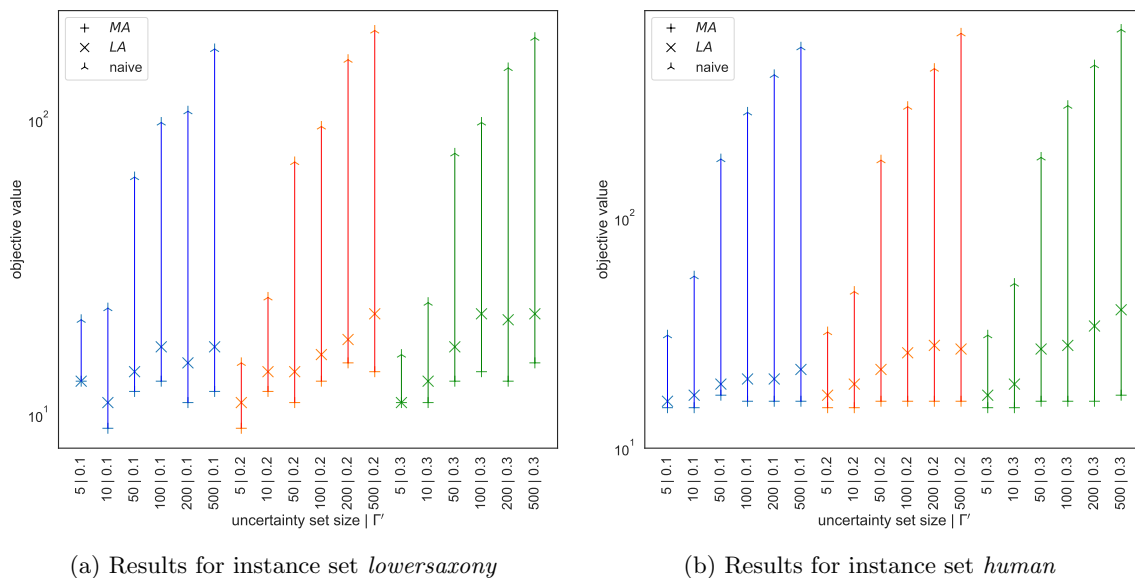


Figure 5: Objective values of *MA*, *LA* and the naive approach for the different uncertainty set sizes $|\mathcal{U}(\Gamma)|$ and values for Γ' (logarithmic scale).

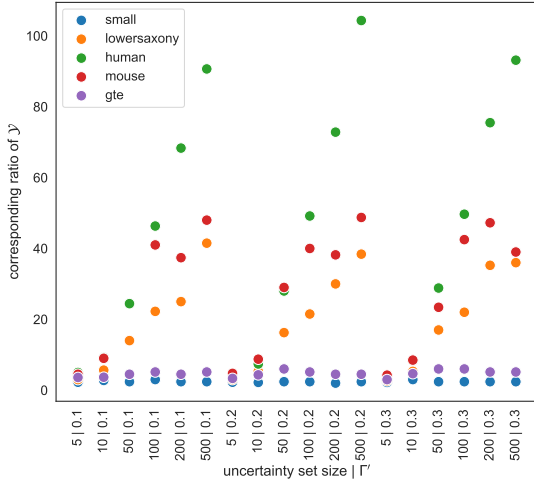
set of paths is generated by the union of the solutions for the individual scenarios, in order to be feasible for all scenarios (as in *LA*), \mathcal{Y} increases with $|\mathcal{U}(\Gamma)|$ (up to a value of 652 and significantly more than in *LA*), which also leads to the objective value being dominated by \mathcal{Y} . This is particularly noticeable with more complex (but not necessarily larger) graphs, where the number of different paths (and thus the objective value) is significantly higher and can be well observed in Figures 5 and 6a. In the latter, one can see how the ratio of the number of paths between the naive approach and *MA* increases significantly for the more complex graphs and with larger values for $|\mathcal{U}(\Gamma)|$ (depending on the instance, the naive approach requires up to 104 times more paths than *MA*). This underlines the advantage of our adjustable models, which provide a substantial improvement compared to the naive approach. Even the less adjustable version *LA* leads to a significant reduction in the number of paths, which can be seen in Figure 6b. It shows the box plots for the five different instance classes. These associated values are calculated from the difference in the number of paths of *LA* and *MA* divided by the difference in the number of paths of the naive approach and *MA*. In other words, it indicates as a percentage how close the \mathcal{Y} value of version *LA* is to the naive approach starting from *MA*. As can be seen in Figure 6b, almost all values are below 0.15. The only exception is instance *gte*, for which the corresponding values range between 0.2 and 0.4, which is still a significant improvement compared to the naive approach.

To summarize the results, it can be noted that the adjustability has a considerable advantage over the non-adjustable model, and this is clearly reflected in the number of paths. Furthermore, even in the less adjustable *LA* case, our models deliver significantly better results than the naive approach at the expense of dealing with more computationally challenging problems.

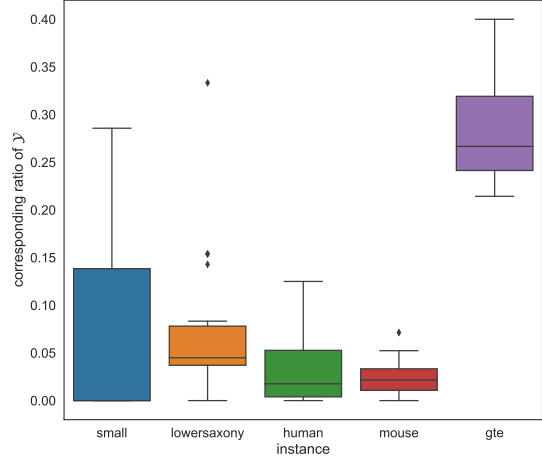
7 Conclusions

In this paper, we address the minimum flow decomposition problem and consider it from the perspective of robust optimization. Unlike typical bioinformatics applications that focus on robustness against measurement errors, we explore classical robustness concepts from the literature. Our primary focus lies on applications related to transportation planning problems, such as optimizing vehicle utilization in public transport.

We demonstrate that both MFDP and MIFDP with interval-wise uncertainty can be reduced to a one-scenario case for strict robustness. As a consequence, we generalize the problem to the weighted inexact case with lower and upper bounds on the flow values. We investigate the complexity of the



(a) \mathcal{Y} of the naive approach divided by \mathcal{Y} of MA for the different uncertainty set sizes $|\mathcal{U}(\Gamma)|$ and values for Γ' , i.e., $\frac{\mathcal{Y}^{\text{naive}}}{\mathcal{Y}^{MA}}$



(b) Difference in \mathcal{Y} of LA and MA divided by the difference in \mathcal{Y} of the naive approach and MA , i.e., $\frac{\mathcal{Y}^{LA} - \mathcal{Y}^{MA}}{\mathcal{Y}^{\text{naive}} - \mathcal{Y}^{MA}}$

Figure 6: Values of $\mathcal{Y} := \sum_i y_i$ of the three algorithms in relation to each other for the different instance sets.

resulting problem and show that we can solve the special case where we only minimize the weights in polynomial time. In addition, we can also show that the other special case, where we only minimize the number of paths, can also be solved in polynomial time if the upper bounds on the flow values are sufficiently large.

Moreover, we introduce the concept of robust flow decomposition by incorporating uncertain flows. We describe how to reduce the strictly robust counterpart to a one-scenario case. Additionally, we show that depending on the objective function weights, special cases can be solved in polynomial time.

To overcome the conservatism of strict robustness, and since it also makes sense from a practical point of view that some decisions can be made after the particular scenario has been observed, we make use of adjustable robustness. Consequently, we present two different adjustable problem formulations. In the first, only the number of paths needs to be specified beforehand. In the second formulation, both the number and the specific paths must be decided before the scenario is revealed. Our subsequent computational study provides a proof of concept, demonstrating the benefits of adjustability in settings under uncertainty when compared to non-adjustable models, which is clearly reflected in the number of paths. Even the less adjustable model yields significantly better results than the approach in which the problem is solved separately for each scenario, and all paths with corresponding weights are aggregated into a pool. Our findings highlight the substantial advantages of our adjustable models. However, the gained flexibility comes at the cost of higher computational requirements. Thus, focusing on specialized solution methods that aim at improving runtimes would be a valuable contribution to future research. In particular, methods that can influence the choice of effective scenarios, both for initializing the algorithm and during its progression, based on external factors (such as data, as proposed in [GK23]) could play a significant role in improving computational performance. Finally, since previous concepts have mainly focused on dealing with data inaccuracies and this is the first work to consider MFDs in the context of classical robustness concepts, this opens up additional fields of application and offers opportunities for further research.

References

[AMO88] Ravindra K Ahuja, Thomas L Magnanti, and James B Orlin. Network flows. 1988.

[BBC11] Dimitris Bertsimas, David B Brown, and Constantine Caramanis. Theory and applications of robust optimization. *SIAM review*, 53(3):464–501, 2011.

- [BK09] Stefan Bunte and Natalia Kliwer. An overview on vehicle scheduling models. *Public Transport*, 1(4):299–317, 2009.
- [BS04] Dimitris Bertsimas and Melvyn Sim. The price of robustness. *Operations research*, 52(1):35–53, 2004.
- [BS07] Hans-Georg Beyer and Bernhard Sendhoff. Robust optimization—a comprehensive survey. *Computer methods in applied mechanics and engineering*, 196(33-34):3190–3218, 2007.
- [BTEGN09] Aharon Ben-Tal, Laurent El Ghaoui, and Arkadi Nemirovski. *Robust optimization*, volume 28. Princeton university press, 2009.
- [BTGGN04] Aharon Ben-Tal, Alexander Goryashko, Elana Guslitzer, and Arkadi Nemirovski. Adjustable robust solutions of uncertain linear programs. *Mathematical programming*, 99(2):351–376, 2004.
- [BTN98] Aharon Ben-Tal and Arkadi Nemirovski. Robust convex optimization. *Mathematics of operations research*, 23(4):769–805, 1998.
- [CQY20] Valentina Cacchiani, Jianguo Qi, and Lixing Yang. Robust optimization models for integrated train stop planning and timetabling with passenger demand uncertainty. *Transportation Research Part B: Methodological*, 136:1–29, 2020.
- [CT12] Valentina Cacchiani and Paolo Toth. Nominal and robust train timetabling problems. *European Journal of Operational Research*, 219(3):727–737, 2012.
- [Die05] Reinhard Diestel. Graph theory 3rd ed. *Graduate texts in mathematics*, 173(33):12, 2005.
- [DT23] Fernando HC Dias and Alexandru I Tomescu. Accurate flow decomposition via robust integer linear programming. *bioRxiv*, pages 2023–03, 2023.
- [DWMT22] Fernando HC Dias, Lucia Williams, Brendan Mumey, and Alexandru I Tomescu. Efficient minimum flow decomposition via integer linear programming. *Journal of Computational Biology*, 29(11):1252–1267, 2022.
- [GH08] Valérie Guihaire and Jin-Kao Hao. Transit network design and scheduling: A global review. *Transportation Research Part A: Policy and Practice*, 42(10):1251–1273, 2008.
- [GK23] Marc Goerigk and Jannis Kurtz. Data-driven robust optimization using deep neural networks. *Computers & Operations Research*, 151:106087, 2023.
- [GMT14] Virginie Gabrel, Cécile Murat, and Aurélie Thiele. Recent advances in robust optimization: An overview. *European journal of operational research*, 235(3):471–483, 2014.
- [GTT89] Andrew V Goldberg, Éva Tardos, and Robert Tarjan. Network flow algorithm. Technical report, Cornell University Operations Research and Industrial Engineering, 1989.
- [HHK⁺12] Tzvika Hartman, Avinatan Hassidim, Haim Kaplan, Danny Raz, and Michal Segalov. How to split a flow? In *2012 Proceedings IEEE INFOCOM*, pages 828–836. IEEE, 2012.
- [HKL05] Dennis Huisman, Leo G Kroon, Ramon M Lentink, and Michiel JCM Vromans. Operations research in passenger railway transportation. *Statistica Neerlandica*, 59(4):467–497, 2005.
- [KY13] Panos Kouvelis and Gang Yu. *Robust discrete optimization and its applications*, volume 14. Springer Science & Business Media, 2013.
- [LFJ11] Wei Li, Jianxing Feng, and Tao Jiang. Isolasso: a lasso regression approach to rna-seq based transcriptome assembly. *Journal of Computational Biology*, 18(11):1693–1707, 2011.
- [LLB18] Richard M Lusby, Jesper Larsen, and Simon Bull. A survey on robustness in railway planning. *European Journal of Operational Research*, 266(1):1–15, 2018.

- [LLER11] Richard M Lusby, Jesper Larsen, Matthias Ehrgott, and David Ryan. Railway track allocation: models and methods. *OR spectrum*, 33:843–883, 2011.
- [LLP12] Chungmok Lee, Kyungsik Lee, and Sungsoo Park. Robust vehicle routing problem with deadlines and travel time/demand uncertainty. *Journal of the Operational Research Society*, 63(9):1294–1306, 2012.
- [LMM⁺23] Eva Ley, Rebecca Marx, Maximilian Merkert, Tim Niemann, and Sebastian Stiller. Robust optimization under controllable uncertainty. 2023.
- [LSBG13] Bingdong Li, Jeff Springer, George Bebis, and Mehmet Hadi Gunes. A survey of network flow applications. *Journal of Network and Computer Applications*, 36(2):567–581, 2013.
- [NH79] Simeon C. Ntafos and S. Louis Hakimi. On path cover problems in digraphs and applications to program testing. *IEEE Transactions on Software Engineering*, (5):520–529, 1979.
- [OKW22] Nils Olsen, Natalia Kliewer, and Lena Wolbeck. A study on flow decomposition methods for scheduling of electric buses in public transport based on aggregated time–space network models. *Central European Journal of Operations Research*, pages 1–37, 2022.
- [Orl88] James Orlin. A faster strongly polynomial minimum cost flow algorithm. In *Proceedings of the Twentieth annual ACM symposium on Theory of Computing*, pages 377–387, 1988.
- [PNP16] Jens Parbo, Otto Anker Nielsen, and Carlo Giacomo Prato. Passenger perspectives in railway timetabling: a literature review. *Transport Reviews*, 36(4):500–526, 2016.
- [SB22] Khodakaram Salimifard and Sara Bigharaz. The multicommodity network flow problem: state of the art classification, applications, and solution methods. *Operational Research*, 22(1):1–47, 2022.
- [Sch12] Anita Schöbel. Line planning in public transportation: models and methods. *OR spectrum*, 34(3):491–510, 2012.
- [Sch14] Anita Schöbel. Generalized light robustness and the trade-off between robustness and nominal quality. *Mathematical Methods of Operations Research*, 80(2):161–191, 2014.
- [SK17] Mingfu Shao and Carl Kingsford. Theory and a heuristic for the minimum path flow decomposition problem. *IEEE/ACM transactions on computational biology and bioinformatics*, 16(2):658–670, 2017.
- [Soy73] Allen L Soyster. Convex programming with set-inclusive constraints and applications to inexact linear programming. *Operations research*, 21(5):1154–1157, 1973.
- [SS22] Philine Schiewe and Moritz Stinzendörfer. Integrated line planning and vehicle scheduling for public transport. In *INOC*, pages 1–6, 2022.
- [SSJ⁺24] Philine Schiewe, Anita Schöbel, Sven Jäger, Sebastian Albert, Christine Biedinger, Thorsten Dahlheimer, Vera Grafe, Sarah Roth, Alexander Schiewe, Felix Spühler, Moritz Stinzendörfer, and Reena Urban. Lintim: An integrated environment for mathematical public transport optimization, 2024.
- [TGP⁺15] Alexandru I Tomescu, Travis Gagie, Alexandru Popa, Romeo Rizzi, Anna Kuosmanen, and Veli Mäkinen. Explaining a weighted dag with few paths for solving genome-guided multi-assembly. *IEEE/ACM transactions on computational biology and bioinformatics*, 12(6):1345–1354, 2015.
- [VCCM08] Benedicte Vatinlen, Fabrice Chauvet, Philippe Chrétienne, and Philippe Mahey. Simple bounds and greedy algorithms for decomposing a flow into a minimal set of paths. *European Journal of Operational Research*, 185(3):1390–1401, 2008.

- [Vel93] Marinus Veldhorst. A bibliography on network flow problems. In *Network Optimization Problems: Algorithms, Applications And Complexity*, pages 301–331. World Scientific, 1993.
- [Way99] Kevin D Wayne. A polynomial combinatorial algorithm for generalized minimum cost flow. In *Proceedings of the thirty-first annual ACM symposium on Theory of computing*, pages 11–18, 1999.
- [WCL18] Hong-Zhi Wei, Chun-Rong Chen, and Sheng-Jie Li. Characterizations for optimality conditions of general robust optimization problems. *Journal of Optimization Theory and Applications*, 177:835–856, 2018.
- [WRM19] Lucia Williams, Gillian Reynolds, and Brendan Mumey. Rna transcript assembly using inexact flows. In *2019 IEEE International Conference on Bioinformatics and Biomedicine (BIBM)*, pages 1907–1914. IEEE, 2019.
- [XRL04] Yi Xing, Alissa Resch, and Christopher Lee. The multiassembly problem: reconstructing multiple transcript isoforms from est fragment mixtures. *Genome research*, 14(3):426–441, 2004.
- [YGdH19] İhsan Yanıkoğlu, Bram L Gorissen, and Dick den Hertog. A survey of adjustable robust optimization. *European Journal of Operational Research*, 277(3):799–813, 2019.
- [ZYGDD11] Xiaoyan Zhu, Qi Yuan, Alberto Garcia-Diaz, and Liang Dong. Minimal-cost network flow problems with variable lower bounds on arc flows. *Computers & Operations Research*, 38(8):1210–1218, 2011.
- [ZZ13] Bo Zeng and Long Zhao. Solving two-stage robust optimization problems using a column-and-constraint generation method. *Operations Research Letters*, 41(5):457–461, 2013.

A Adjustable formulations

A.1 Master problem and sub-problem for *MA*

Formulations of the master problem (20) and sub-problem (21) for *MA* in Algorithm 1 in Section 5.

$$\min_{x, y, w} \sum_{i=1}^{\bar{K}} y_i + \mathcal{W} \quad (20a)$$

$$\text{s.t.} \quad \sum_{i=1}^{\bar{K}} w_i^\xi \leq \mathcal{W}, \quad \forall \xi \in \bar{\mathcal{U}}, \quad (20b)$$

$$\sum_{v:(s,v) \in E} x_{svi}^\xi = y_i, \quad \forall i \in \{1, \dots, \bar{K}\}, \xi \in \bar{\mathcal{U}}, \quad (20c)$$

$$\sum_{u:(u,t) \in E} x_{uti}^\xi = y_i, \quad \forall i \in \{1, \dots, \bar{K}\}, \xi \in \bar{\mathcal{U}}, \quad (20d)$$

$$\sum_{(u,v) \in E} x_{uvi}^\xi - \sum_{(v,w) \in E} x_{vwi}^\xi = 0, \quad \forall i \in \{1, \dots, \bar{K}\}, v \in V \setminus \{s, t\}, \xi \in \bar{\mathcal{U}}, \quad (20e)$$

$$\sum_{i \in \{1, \dots, \bar{K}\}} w_i^\xi x_{uvi}^\xi \geq f_{uv}^{l, \xi}, \quad \forall (u, v) \in E, \xi \in \bar{\mathcal{U}}, \quad (20f)$$

$$\sum_{i \in \{1, \dots, \bar{K}\}} w_i^\xi x_{uvi}^\xi \leq f_{uv}^{u, \xi}, \quad \forall (u, v) \in E, \xi \in \bar{\mathcal{U}}, \quad (20g)$$

$$\mathcal{W} \in \mathbb{Z}^+, \quad (20h)$$

$$w_i^\xi \in \mathbb{Z}^+, \quad \forall i \in \{1, \dots, \bar{K}\}, \xi \in \bar{\mathcal{U}}, \quad (20i)$$

$$x_{uvi}^\xi \in \{0, 1\}, \quad \forall (u, v) \in E, i \in \{1, \dots, \bar{K}\}, \xi \in \bar{\mathcal{U}}, \quad (20j)$$

$$y_i \in \{0, 1\}, \quad \forall i \in \{1, \dots, \bar{K}\}. \quad (20k)$$

$$\min_{x, y, w} \sum_{i=1}^{\bar{K}} y_i + \mathcal{W} \quad (21a)$$

$$\text{s.t.} \quad \sum_{i=1}^{\bar{K}} w_i^\xi \leq \mathcal{W}, \quad \forall \xi \in \mathcal{U}, \quad (21b)$$

$$\sum_{v:(s,v) \in E} x_{svi}^\xi = y_i, \quad \forall i \in \{1, \dots, \bar{K}\}, \xi \in \mathcal{U}, \quad (21c)$$

$$\sum_{u:(u,t) \in E} x_{uti}^\xi = y_i, \quad \forall i \in \{1, \dots, \bar{K}\}, \xi \in \mathcal{U}, \quad (21d)$$

$$\sum_{(u,v) \in E} x_{uvi}^\xi - \sum_{(v,w) \in E} x_{vwi}^\xi = 0, \quad \forall i \in \{1, \dots, \bar{K}\}, v \in V \setminus \{s, t\}, \xi \in \mathcal{U}, \quad (21e)$$

$$\sum_{i \in \{1, \dots, \bar{K}\}} w_i^\xi x_{uvi}^\xi \geq f_{uv}^{l, \xi}, \quad \forall (u, v) \in E, \xi \in \mathcal{U}, \quad (21f)$$

$$\sum_{i \in \{1, \dots, \bar{K}\}} w_i^\xi x_{uvi}^\xi \leq f_{uv}^{u, \xi}, \quad \forall (u, v) \in E, \xi \in \mathcal{U}, \quad (21g)$$

$$\mathcal{W} \in \mathbb{Z}^+, \quad (21h)$$

$$w_i^\xi \in \mathbb{Z}^+, \quad \forall i \in \{1, \dots, \bar{K}\}, \xi \in \mathcal{U}, \quad (21i)$$

$$x_{uvi}^\xi \in \{0, 1\}, \quad \forall (u, v) \in E, i \in \{1, \dots, \bar{K}\}, \xi \in \mathcal{U}. \quad (21j)$$

A.2 Adjustable formulation *LA*

Adjustable MIP formulation (22) for *LA* in Section 5, where the wait-and-see variables w^ξ depend on the scenario $\xi \in \mathcal{U}$ (given by the bounds $f^{l, \xi}$ and $f^{u, \xi}$).

$$\min_{x, y, w} \sum_{i=1}^{\bar{K}} y_i + \mathcal{W} \quad (22a)$$

$$\text{s.t.} \quad \sum_{i=1}^{\bar{K}} w_i^\xi \leq \mathcal{W}, \quad \forall \xi \in \mathcal{U}, \quad (22b)$$

$$\sum_{v:(s,v) \in E} x_{svi} = y_i, \quad \forall i \in \{1, \dots, \bar{K}\}, \quad (22c)$$

$$\sum_{u:(u,t) \in E} x_{uti} = y_i, \quad \forall i \in \{1, \dots, \bar{K}\}, \quad (22d)$$

$$\sum_{(u,v) \in E} x_{uvi} - \sum_{(v,w) \in E} x_{vwi} = 0, \quad \forall i \in \{1, \dots, \bar{K}\}, v \in V \setminus \{s, t\}, \quad (22e)$$

$$\sum_{i \in \{1, \dots, \bar{K}\}} w_i^\xi x_{uvi} \geq f_{uv}^{l, \xi}, \quad \forall (u, v) \in E, \xi \in \mathcal{U}, \quad (22f)$$

$$\sum_{i \in \{1, \dots, \bar{K}\}} w_i^\xi x_{uvi} \leq f_{uv}^{u, \xi}, \quad \forall (u, v) \in E, \xi \in \mathcal{U}, \quad (22g)$$

$$\mathcal{W} \in \mathbb{Z}^+, \quad (22h)$$

$$w_i^\xi \in \mathbb{Z}^+, \quad \forall i \in \{1, \dots, \bar{K}\}, \xi \in \mathcal{U}, \quad (22i)$$

$$x_{uvi} \in \{0, 1\}, \quad \forall (u, v) \in E, i \in \{1, \dots, \bar{K}\}, \quad (22j)$$

$$y_i \in \{0, 1\}, \quad \forall i \in \{1, \dots, \bar{K}\}. \quad (22k)$$

The corresponding column-and-constraint generation approach (based on [ZZ13]) to solve the adjustable problem *LA* in (22) can be found in Algorithm 3.

As described in Section 5, if a given solution (y^k, x^k) for the master problem leads to an infeasible sub-problem, we know that we can eliminate the combination of (y^k) and (x^k) from the solution space. As a consequence, in line 13 of Algorithm 3, we add the corresponding constraint to the master problem (23).

Algorithm 3: Column-and-constraint generation method for LA

```

1 given a scenario set  $\mathcal{U}$  and threshold  $\epsilon$ ;
2 Set  $LB = -\infty, UB = \infty, k = 1$  and initialize  $\bar{\mathcal{U}}$  with one scenario from  $\mathcal{U}$ ;
3 while  $UB - LB > \epsilon$  do
4   solve master problem (23), get optimal solution  $(y^k, x^k, w^k, \mathcal{W}^k)$ ;
5   update lower bound  $LB = \sum_{i=1}^{\bar{K}} (y^k)_i + \mathcal{W}^k$ ;
6   solve sub-problem (24) with input  $(y^k, x^k)$ ;
7   if we get optimal solution  $(\bar{w}^k, \bar{\mathcal{W}}^k)$  then
8     let  $\xi^k$  be the worst-case scenario causing  $\bar{\mathcal{W}}^k$ ;
9     update upper bound  $UB = \sum_{i=1}^{\bar{K}} (y^k)_i + \bar{\mathcal{W}}^k$ ;
10  end
11  else
12    let  $\xi^k$  be the first scenario causing infeasibility;
13    add  $\sum_{i:(y^k)_i=0} y_i + \sum_{i:(x^k)_i=0} x_i + \sum_{i:(y^k)_i=1} (1 - y_i) + \sum_{i:(x^k)_i=1} (1 - x_i) \geq 1$  to
      constraints of master problem (23);
14  end
15  add  $\xi^k$  to  $\bar{\mathcal{U}}$ ;
16   $k = k + 1$ ;
17 end
18 return  $(y^k, x^k, \bar{w}^k)$ ;

```

The described master problem and sub-problem of LA in Algorithm 3 are shown in (23) and (24), respectively.

$$\min_{x, y, w} \sum_{i=1}^{\bar{K}} y_i + \mathcal{W} \quad (23a)$$

$$\text{s.t.} \quad \sum_{i=1}^{\bar{K}} w_i^\xi \leq \mathcal{W}, \quad \forall \xi \in \bar{\mathcal{U}}, \quad (23b)$$

$$\sum_{v:(s,v) \in E} x_{sv} = y_i, \quad \forall i \in \{1, \dots, \bar{K}\}, \quad (23c)$$

$$\sum_{u:(u,t) \in E} x_{ut} = y_i, \quad \forall i \in \{1, \dots, \bar{K}\}, \quad (23d)$$

$$\sum_{(u,v) \in E} x_{uv} - \sum_{(v,w) \in E} x_{vw} = 0, \quad \forall i \in \{1, \dots, \bar{K}\}, v \in V \setminus \{s, t\}, \quad (23e)$$

$$\sum_{i \in \{1, \dots, \bar{K}\}} w_i^\xi x_{uv} \geq f_{uv}^{l,\xi}, \quad \forall (u, v) \in E, \xi \in \bar{\mathcal{U}}, \quad (23f)$$

$$\sum_{i \in \{1, \dots, \bar{K}\}} w_i^\xi x_{uv} \leq f_{uv}^{u,\xi}, \quad \forall (u, v) \in E, \xi \in \bar{\mathcal{U}}, \quad (23g)$$

$$\mathcal{W} \in \mathbb{Z}^+, \quad (23h)$$

$$w_i^\xi \in \mathbb{Z}^+, \quad \forall i \in \{1, \dots, \bar{K}\}, \xi \in \bar{\mathcal{U}}, \quad (23i)$$

$$x_{uv} \in \{0, 1\}, \quad \forall (u, v) \in E, i \in \{1, \dots, \bar{K}\}, \quad (23j)$$

$$y_i \in \{0, 1\}, \quad \forall i \in \{1, \dots, \bar{K}\}. \quad (23k)$$

$$\min_{x, y, w} \sum_{i=1}^{\bar{K}} y_i + \mathcal{W} \quad (24a)$$

$$\text{s.t.} \quad \sum_{i=1}^{\bar{K}} w_i^\xi \leq \mathcal{W}, \quad \forall \xi \in \mathcal{U}, \quad (24b)$$

$$\sum_{i \in \{1, \dots, \bar{K}\}} w_i^\xi x_{uv} \geq f_{uv}^{l,\xi}, \quad \forall (u, v) \in E, \xi \in \mathcal{U}, \quad (24c)$$

$$\sum_{i \in \{1, \dots, \bar{K}\}} w_i^\xi x_{uv} \leq f_{uv}^{u,\xi}, \quad \forall (u, v) \in E, \xi \in \mathcal{U}, \quad (24d)$$

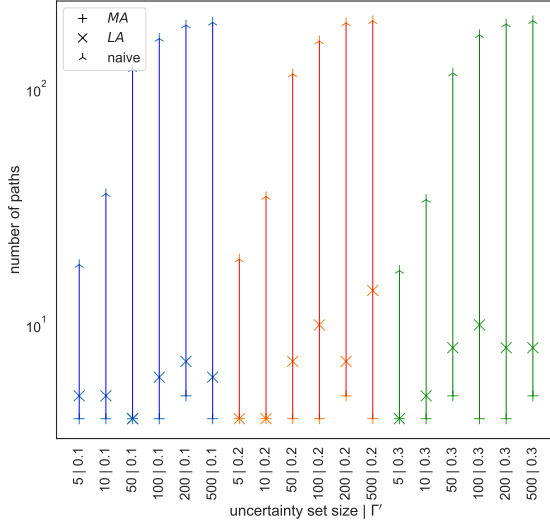
$$\mathcal{W} \in \mathbb{Z}^+, \quad (24e)$$

$$w_i^\xi \in \mathbb{Z}^+, \quad \forall i \in \{1, \dots, \bar{K}\}, \xi \in \mathcal{U}. \quad (24f)$$

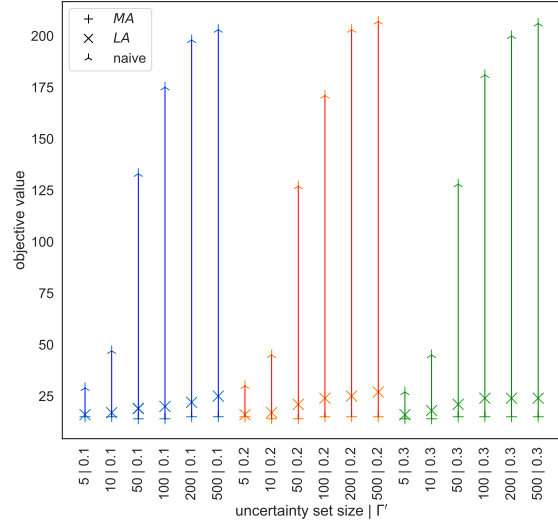
B Detailed Results

Complementing Section 6.2, the remaining results can be found in the following. For *mouse* and *gte*, Figures 7 and 8 show both the values for $\mathcal{Y} := \sum_i y_i$ and the objective values for the different uncertainty set sizes and values for Γ .

The values for \mathcal{Y} for *lowersaxony* and *human* are shown in Figures 9a and 9b, respectively.

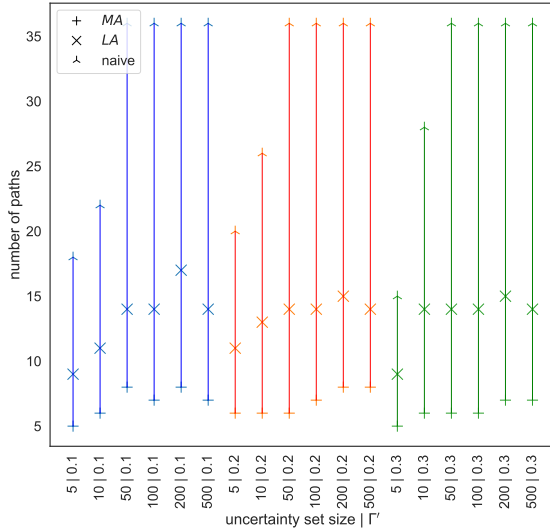


(a) Values of \mathcal{Y} (logarithmic scale)

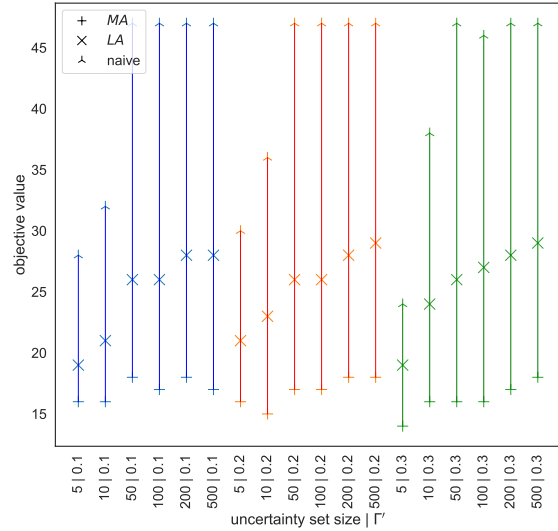


(b) Objective values

Figure 7: Results of *MA*, *LA* and the naive approach for instance set *mouse* for the different uncertainty set sizes $|\mathcal{U}(\Gamma)|$ and values for Γ' .

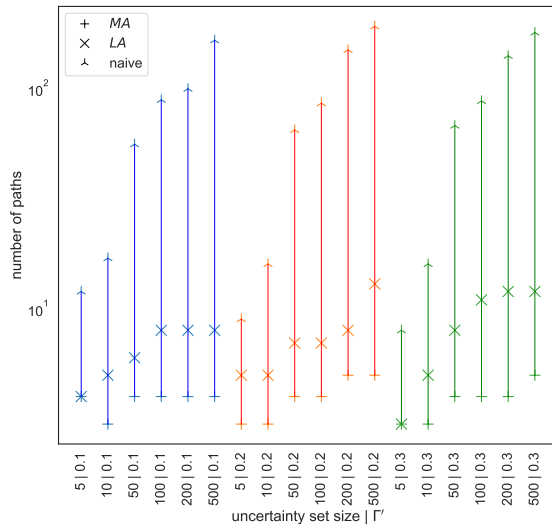


(a) Values of \mathcal{Y}

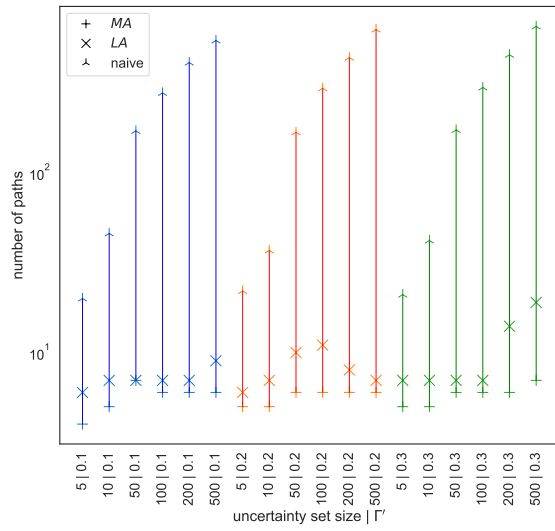


(b) Objective values

Figure 8: Results of *MA*, *LA* and the naive approach for instance set *gte* for the different uncertainty set sizes $|\mathcal{U}(\Gamma)|$ and values for Γ' .



(a) Results for instance set *lowersaxony*



(b) Results for instance set *human*

Figure 9: Values for \mathcal{Y} of *MA*, *LA* and the naive approach for the different uncertainty set sizes $|\mathcal{U}(\Gamma)|$ and values for Γ' (logarithmic scale).